Supplementary Materials for

Interacting Amino Acid Replacements Allow Poison Frogs to Evolve Epibatidine Resistance

Rebecca D. Tarvin[1,*,†], Cecilia M. Borghese[2,†], Wiebke Sachs[2,3,‡], Juan C. Santos[4], Ying Lu[1], Lauren A. O'Connell[5], David C. Cannatella[1,6], R. Adron Harris[2], and Harold H. Zakon[1].

correspondence to: rdtarvin@gmail.com

This PDF file includes:

Materials and Methods
Supplementary Text
Fig S1 to S4
Table S1 to S16
Captions for databases S1 to S2

Other Supplementary Materials for this manuscript includes the following:

Databases S1 to S2 as zipped archives:
Chrnb2_alignment.nex, Chrna4_alignment.nex

Materials and Methods

Specimen Collection

Individuals were collected by JCS and LAO in Ecuador in 2013 under Ecuadorian permit No. 003-11 IC-FAU-DNB/MA to Luis A. Coloma and by RDT under Texas Parks and Wildlife Department Permit No. SPR-1097-912 to Travis Laduc (see supplementary table S1 for collection sites and species). Animals were euthanized with benzocaine (Orajel® dental gel) under ethically approved protocols (Harvard University IACUC # 12-10, UT Austin IACUC # 2012-00032); tissue samples of brain and muscle were removed and stored in RNAlater® (Life Technologies, Carlsbad, CA) at –20°C.

RNA Library Preparation, Transcriptome and nAChR Gene Assembly

Trizol (Life Technologies, Carlsbad, CA) was used to extract total RNA; rRNA was removed with the Poly(A) Purist kit (Life Technologies, Carlsbad, CA). Libraries of mRNA with RNA integrity numbers (RIN) $\geq$ 8.0 were prepared with the NEXTflex directional RNA-Seq dUTP-based kit (Bioo Scientific, Austin, TX). Following barcoding of cDNA libraries, 10-18 cycles of PCR were used to enrich cDNA. The resulting cDNA libraries were quantified and qualitatively analyzed with Bioanalyzer 2500 (Agilent Technologies, CA) and purified using AMPure XP beads (Beckman Coulter, Inc) to a total mean size of 300 bp. Libraries were sequenced with 100 bp paired-end sequencing on the Illumina HiSeq 2100 platform at the UT Austin Genomic Sequencing and Analysis Facility.

Raw sequences were evaluated using FastQC v 0.10.1 (*37*); low-quality reads were removed or trimmed using SnoWhite v 2.0.3 (*38*, *39*) with default parameters except: -Q 20, -D T, -L T, -Y T, -a B, -t B, -b 6, -I 20. A custom script was used to verify that sequence reads were present in both paired-end files. These reads were then assembled into de novo transcriptomes with Trinity v2013-02-25, using default Trinity parameters for strand specific paired data (--SS_lib_type RF) (*40*, *41*). Assemblies were run on large memory nodes of the Lonestar cluster at the Texas Advanced Computing Center (TACC). BLASTX (*42*) was used to compare the transcriptomes to the Universal Protein Resource (UniProt) database (*43*).

We used transcripts that matched Chrnb2 and Chrna4 genes with an *E* value cutoff of 10^{-5} to reconstruct more complete gene sequences for the other frog transcriptomes using MITO_bim (*44*). This program iteratively baits and assembles cleaned Illumina reads on a reference sequence. We used default parameters for MITO_bim as well as the additional options '--clean' and '--quick'. When paired end reads were available, we interleaved them and used the '--paired' option. For reads that were longer than 75 bp, we used a longer kmer ('-kbait 45'); otherwise we used the default -kbait of 31 bp. Outgroup sequences were obtained directly from Genbank or were reconstructed from SRA entries as described above. Specimen information can be found in table S1.

AA Replacement Identification

We aligned gene assemblies using the linsi algorithm in MAFFT v7.023b (*45*) and adjusted the alignment to match the start and end codon of *Homo sapiens* CHRNB2 and CHRNA4 proteins (NCBI accession numbers NM_000748.2 and NM_000744.6, respectively). To place our sequences in an evolutionary context, we compared sequences across dendrobatid frogs, non-dendrobatid frogs, and several non-frog outgroups using

the reference phylogeny as described in (*15*) (see table S4 for GenBank accession numbers). We reviewed the alignment site by site to identify residues that were highly conserved in non-dendrobatid frogs and other vertebrates, but showed patterns of AA replacements that were associated with epibatidine chemical defense in dendrobatids, which is known only from species of the *Epipedobates* and *Ameerega* clades. We identified four sites in Chrnb2 and one site in Chrna4 that were caused by a mutation in the first or second codon position and appeared to be associated with epibatidine defense.

To improve our phylogenetic sampling, we designed primers from the reconstructed genes and sequenced the identified region in Chrnb2 from additional samples from the Genetic Diversity Collection of UT Biodiversity Collections (see supplementary table S1 for species and museum numbers) and recent tissue collections (under permit IBD0359 - Res 1177-2014 [Colombia]) Primers that were used are: chrnb2-Cfug-413F (5'-AAGTGCGTCTCCCATCCAAG-3') and chrnb2-Cfug-814R (5'-TGTAGAACAGAGGCTTGCGG-3'). PCR parameters were: 4-min initial denaturation at 93°C, 40 cycles of 30 s at 93°C, 30 s at 60°C, 45 s at 72°C, and a final extension time of 7 min at 72°C. PCR products were sequenced using forward and reverse primers at the UT Austin Institute for Cellular and Molecular Biology Core Facility on an Applied Biosystems 3730 DNA Sequencer. The sequences reported are only reverse reads because the forward primer was located on the edge of a long intron that varied in length and did not produce readable sequences.

In Vitro Transcription

cDNAs encoding human nAChR subunits were cloned in pSP64 (constructs generously shared by Dr. J. M. Lindstrom). cDNAs encoding *Epipedobates* nAChR subunits were synthesized, optimized for expression in *Xenopus laevis* and subcloned in pGEMHE by GenScript (Piscataway, NJ). After linearizing the plasmids, the *in vitro* transcription of nAChR subunits was performed using mMessage mMachine (Life Technologies, Grand Island, NY).

Oocyte Isolation and Injection

Xenopus laevis frogs were obtained from Nasco (Fort Atkinson, WI) and cared for according to the recommendations of the NIH Guide for the Care and Use of Laboratory Animals. All surgery was performed in accordance with protocols approved by the University of Texas, Austin IACUC (AUP-2015-00205 and AUP-2016-00016). Part of *X. laevis* ovaries were surgically removed from a frog and placed in Isolation media (108 mM NaCl; 2 mM KCl; 1 mM EDTA; 10 mM HEPES; pH = 7.5). The oocytes were then manually isolated and treated with 0.5 mg/ml collagenase for 10 min. Thereafter, cRNA encoding the nAChR subunits (for human subunits: 10 ng total cRNA, α4:β2 in 1:3 or 3:1 W/W ratios; for *Epipedobates* subunits: 32 or 40 ng total cRNA, α4:β2 in 1:7 or 7:1 W/W ratios) was injected with the Nanoject II (Drummond Scientific Company, Broomall, PA) into the cytoplasm of the oocytes. The injected oocytes were kept at 16°C in incubation media (composition: 50 % Leibovitz L-15 medium; 10 mM HEPES; 10 U/ml penicillin; 10 μg/ml streptomycin; pH = 7.4).

Chemicals

All chemicals and solvents were of analytical grade and were purchased from Sigma-Aldrich (St. Louis, MO), Mallinckrodt Chemicals (St. Louis, MO), Amresco (Solon, OH) and Life Technologies (Grand Island, NY). Epibatidine was purchased from Tocris Bioscience (Bio-Techne, Minneapolis, MN).

Electrophysiological Recordings

Responses to ACh and epibatidine were studied 1-10 days after injection through two-electrode voltage-clamp (Oocyte Clamp OC-725C, Warner Instruments, Hamden, CT), and digitized using a PowerLab 4/30 system (ADInstruments, Colorado Springs, CO). The oocytes were placed in a rectangular chamber and continuously perfused with Ba-ND96 + Atropine buffer (2 ml/min; 96 mM NaCl, 2 mM KCl, 1 mM $BaCl_2$, 1 mM $MgCl_2$, 10 mM HEPES, 1 μM atropine) at room temperature. Oocytes were clamped at -70 mV using two glass electrodes filled with 3 M KCl. All drugs were applied by bath-perfusion, and solutions were prepared the day of the application.

Concentration-response curves (CRCs) for acetylcholine (ACh) and epibatidine were obtained by applying increasing concentrations (20-30 s applications for ACh, 30-120 s for epibatidine) with 5-20 min washout times. All responses were normalized to the maximal ACh response seen in that oocyte by assigning it a 100% value. Oocytes with currents larger than 20 μA were discarded.

Statistical Analysis

Results were expressed as mean ± SEM. All statistical analysis was performed with Prism 7 (GraphPad Software Inc., San Diego, CA). The results from the CRCs were fitted to monophasic (Eq. 1) or biphasic (Eq. 2) logistic equations, and all parameters (log EC_{50}, Hill coefficients, maximal currents) were determined. The best fitted equation was determined by applying the Extra sum-of-squares F test. All relevant CRC results and parameters are shown in tables S5−S8.

$$I = \frac{Maximal\ current}{1+10^{(logEC_{50}-\log[agonist])\times n_H}} \qquad \text{Eq. 1}$$

$$I = \frac{Maximal\ current_A}{1+10^{(logEC_{50A}-\log[agonist])\times n_{HA}}} + \frac{Maximal\ current_B}{1+10^{(logEC_{50B}-\log[agonist])\times n_{HB}}} \qquad \text{Eq. 2}$$

I, measured current; *Maximal current* achieved, expressed as a percentage of the maximal ACh response recorded in that oocyte; EC_{50}, effective concentration 50, or concentration that produces half the maximal current; n_H, Hill coefficient. Subscripts A and B indicate correspondence to two different populations of responses.

Two-way analysis of variance (ANOVA) corrected for multiple comparisons with Sidak's test was used to compare $logEC_{50}$ and *Maximal Currents* within each group of results whenever possible (Human-to-*Epipedobates*, tables S9-S10; Human-to-*Ameerega*, tables S11-S12; *Epipedobates*-to-Human, tables S13-S15). The ACh responses from nAChRs containing either human (*H*) or *Epipedobates* (*E*) subunits or their combination in an α4:β2 cRNA ration of 7:1 were best-fitted by mono- or biphasic curves. The high sensitivity component of the biphasic curves is associated with a very high error, because it comprises a smaller proportion of the receptors and the slope of the curve is small.

Therefore, only the $logEC_{50}$ values from the monophasic and the low sensitivity portion (b) of the biphasic curves were considered in the one-way ANOVA (table S16).

Supplementary Text

Double Mutants in Human-to-*Ameerega* High-Sensitivity nAChRs

In these experiments we aimed to verify the effects of mutation combinations, which are not always predictable. While usually the result is the sum of individual effects, in some cases one mutation dominates over the other, and in a small percentage of cases, the interaction causes completely unpredictable outcomes.

For example, the F**C**A**V** genotype did not seem to modify the ACh sensitivity compared with the FSAI genotype (fig. S3A), even though it includes the S108C and the I118V replacements, which by themselves (F**C**AI and FSA**V** genotypes) induce the appearance of a biphasic curve (suggesting the presence of a LS binding site) (fig 2C). In the other two double mutants F**CV**I and FS**VV**, sensitivity to ACh appeared to decrease, similar to the effect of the individual single mutants (F**C**AI and FSA**V**) (fig. S3A, tables S6 and S9).

There were also interactions among the effects on epibatidine resistance of three AA replacements in *Ameerega* (fig. S3B and table S6). In all three double mutants, sensitivity to epibatidine decreased, likely conferred by either the S108C and/or the I118V replacement, which both individually increase the epibatidine EC_{50} values (table S11). However, the normalized maximal epibatidine response was increased in the FS**VV** genotype compared with the FSAI genotype, while none of the single mutants showed an increased normalized maximal epibatidine response (table S12). Therefore, in some cases, the combination of the AA in the same subunit affected the epibatidine action on nAChR function in ways unpredicted by the single AA replacements.

Low-ACh-sensitivity nAChR

When the ratio of injected α4:β2 cRNA was reversed to 3:1, which should favor the formation of the LS stoichiometry $(\alpha4)_3(\beta2)_2$, the ACh sensitivity decreased as expected. In these cases, the best fit for the ACh currents was usually a biphasic curve consisting of high- and low-sensitivity populations (HS and LS, respectively). The appearance of a second population is due to the presence of a non-canonical binding site at the α^+–α^- interface (*46*, *47*), which denotes the LS $(\alpha4)_3(\beta2)_2$ receptors. For some currents, it was not possible to fully discriminate the two populations, observing instead a "flat" (low Hill coefficient) single population curve.

Results from electrophysiology of the LS nAChR were not as clear as those from the HS receptors. It is possible that there were HS receptors present, even though the ratio favors the formation of LS receptors, and this complicates the evaluation. Human-to-frog genotypes (F**C**AI, **LC**AI and F**CVV**) showed decreased sensitivity to ACh compared to wild-type human receptors (FSAI) (fig. S2A and 2C), mainly because they lacked the HS component (i.e., the left part of the biphasic curve). Overall, both stoichiometries of the human-to-frog nAChRs showed lower sensitivity to epibatidine compared to that of the human genotype (FSAI) (fig. S2B and 2D and table S9). Similar to the HS nAChRs, the change in sensitivity to epibatidine in the LS nAChR was driven by the S108C mutation (F**C**AI genotype), which was present in all three frog clades, in addition to the I118V

replacement, which was present only in *Ameerega* (fig. S2B and 2D and table S9). The other mutations (F106L in *Epipedobates* and A110V in *Ameerega*) appeared to correct (at least partially) the decrease in ACh sensitivity induced by the epibatidine-insensitive replacements. As previously reported (*26*), we observed that epibatidine is a super-agonist in the low sensitivity nAChRs, i.e., it elicits maximal currents larger than those induced by a maximal concentration of ACh, the endogenous ligand (see human α4β2 nAChR FSAI genotype, Fig. S2B). While the epibatidine super-agonist activity is present in the 3:1 F**C**AI receptors, it did not reach the levels of the other genotypes in the group, likely because the presence of the Cys interferes with the epibatidine binding.

Unexpected Formation of LS Stoichiometry in Mutant Human nAChR

In the human-to-frog F**C**AI genotype receptors that formed following the injection ratio of 1α:3β, which should favor the HS stoichiometry, a low sensitivity ACh component appears unexpectedly, producing a biphasic curve (Fig. 2A). There are three hypotheses that could explain this. 1) There is a β^+–β^- interface in HS $(\alpha4)_2(\beta2)_3$ receptors which the S108C mutation modifies in such a way that it now binds ACh at a lower sensitivity, similar to the low sensitivity binding site at the α^+–α^- interface of LS $(\alpha4)_3(\beta2)_2$ receptors. As all the AAs required for the ACh binding site in the primary (+) side of the interface are present in the β2 subunit, this would require only a change in the complementary (–) side, where C108 is located. 2) The two α^+–β^- binding sites are not functionally equivalent, as the β2 subunits are flanked one by an α4 and the other by a β2 subunit (*48*). Replacing S108 with Cys could enhance those differences until one binding site has a much lower ACh sensitivity than the other, producing biphasic CRCs. 3) S108, along with the other three AA replacements, is located in a region homologous to the one critical for surface expression of muscle nAChRs (*49*). Other mutations have been shown to modify the stoichiometry of the nAChR (*50*, *51*), so the substitution of S108 by Cys could affect the assembly/trafficking of the nAChR, enabling the formation of LS $(\alpha4)_3(\beta2)_2$ receptors even though the cRNA ratio favors the other stoichiometry.

In support of the third hypothesis, the epibatidine CRCs are basically identical for the 1:3 and 3:1 F**C**AI genotype in human receptors (parameters in Table S5, statistics in Table S9 and S10), suggesting that both 1:3 and 3:1 F**C**AI genotypes assemble in the LS stoichiometry. Moreover, the ACh CRC of the 1:3 and 3:1 F**C**AI nAChR are remarkably similar (table S5). In contrast, epibatidine and ACh CRCs of genotypes not containing the Cys (FSAI and **L**SAI) differ between 1:3 and 3:1 ratios in ACh EC_{50}, epibatidine EC_{50} and normalized maximal current (tables S5, S9 and S10), suggesting that they are capable of forming HS and LS stoichiometry.

Epipedobates-to-Human and Human-frog Combination Receptors

Our results suggest that the *Epipedobates* nAChR may not be able to form the LS $(\alpha4)_3(\beta2)_2$ receptors, at least when expressed in *Xenopus* oocytes. As previously mentioned, this stoichiometry normally possesses a lower ACh sensitivity binding site due to the α^+-α^- interface in $(\alpha4)_3(\beta2)_2$. Even when we increased the α:β cRNA ratio to 7:1, the ACh CRCs were indistinguishable from the 1:7 counterparts (tables S7 and S13). In contrast to the human nAChRs, the ACh responses of 7:1 *Epipedobates* receptors showed monophasic HS CRCs (Fig. S2G, table S7), not the right shifted or biphasic ACh CRCs that are characteristic of the $(\alpha4)_3(\beta2)_2$ nAChR stoichiometry (Fig. S2A and S2C,

table S5). The sensitivity to ACh was the same for all 7:1 *Epipedobates* nAChRs; the only difference arose between LCAI and **F**CAI genotypes, where **F**CAI was less sensitive than LCAI (tables S7 and S13). The epibatidine CRCs presented a pattern of changes similar to the one observed for the high-sensitivity nAChRs (Fig 2H versus fig. S2H; tables S7 and S14), where **FS**AI and L**S**AI genotypes showed high sensitivity to epibatidine, while LCAI and **F**CAI exhibited low sensitivity to the toxin. All epibatidine EC_{50} values were slightly increased in the 7:1 compared to the 1:7 receptors (tables S7 and S14), but the increase was nowhere near the changes observed between the 1:3 and 3:1 human receptors.

To further investigate the possibility that *Epipedobates* nAChR do not form the LS $(\alpha4)_3(\beta2)_2$ stoichiometry, we injected combinations of human and *Epipedobates* subunits in the 7:1 α:β ratio (fig. S4, tables S8 and S16). When the human α4 subunit was expressed with the human β2, the usual two-population CRC was observed, corresponding to the LS $(\alpha4)_3(\beta2)_2$ stoichiometry; when it was co-injected with the *Epipedobates* β2 (LCAI) subunit, the result was a CRC intermediate between the *Epipedobates* and the human nAChRs, with a low Hill coefficient, where both stoichiometries appeared to be present but the currents could not be resolved in two populations. Therefore, when *Epipedobates* β2(LCAI) subunits were co-expressed with human α4, they were capable of forming the LS $(\alpha4)_3(\beta2)_2$ stoichiometry, although not as efficiently as the human β2(FSAI). In contrast, every subunit combination containing the *Epipedobates* α4 subunit produced only HS nAChRs, suggesting that any receptor with this subunit was only capable of forming the HS $(\alpha4)_2(\beta2)_3$ stoichiometry. Thus, the main determinant for the formation of the LS $(\alpha4)_3(\beta2)_2$ stoichiometry in these frogs is the α4 subunit.

Alignment of the α4 sequences (table S3) showed an AA that differs between *Epipedobates* (N176) and all other dendrobatid species sequenced (where that AA is D). This AA is proximal to the epibatidine binding site at the α4-α4 interface, but not in direct contact with epibatidine (see fig. S1 for localization of the AA in the complementary side of the interface). We tested the corresponding mutants to determine if this AA was sufficient [*Epipedobates* α4(N176D) replacement, α4(**D**) genotype] or necessary [human α4(D176N) replacement, α4(**N**) genotype] to allow the formation of LS receptors when co-expressed with the corresponding wild-type β2. None of these manipulations modified the CRCs compared with the respective wild-types. Therefore, the inability to form the LS nAChR likely depends on additional mutations present in the α4 subunit, and, to a lesser degree, on others present in the β2 subunit besides the ones studied here. As the number of AAs different in *Epipedobates* α4 from the human receptors proximal to the α-α interface is quite high, we were unable to determine the identity of the AA responsible for this characteristic (see table S3). The α4 AA replacement in *Epipedobates* (α4N176) is located at the complementary side of the interface, and it could only be proximal to the epibatidine binding site in LS $(\alpha4)_3(\beta2)_2$ receptors. As the *Epipedobates* α4 subunits only form HS nAChRs, no matter the β2 subunit co-expressed, we did not study the epibatidine actions on the α4(N176D)-containing receptors.

As the AAs present in β2 that drive the formation of HS nAChRs seem to be less critical than those in α4, we wondered whether the FCAI genotype would be able to form LS nAChRs when co-expressed with human α4. In the human nAChRs, the β2(F**C**AI)

genotype induced a biphasic ACh CRC, even when injected in the 1:3 ratio, which favors formation of the HS nAChR. When human α4 subunits were co-expressed with *Epipedobates* β2(**F**CAI) subunits, the resulting ACh CRC was biphasic like the human α4β2(FSAI), in contrast to the monophasic, "flat" curve obtained with human α4 *Epipedobates* β2(LCAI). Therefore, the *Epipedobates* β2(LCAI) subunit is clearly capable of forming LS $(\alpha4)_3(\beta2)_2$ receptors when partnered with some unknown, critical AA present in the human α4 subunit, and that capability is greatly improved with the β2(**F**CAI) genotype. However, the FCAI genotype carries a cost in the poison frog HS $(\alpha4)_2(\beta2)_3$ receptors (2-fold decrease in ACh sensitivity, Table 1), and therefore may require compensatory mutations to balance this trade off. We were able to identify at least some of these additional replacements in *Epipedobates* and *Ameerega*. *Oophaga* may possess other unidentified mechanisms or mutations that allow the FCAI genotype to survive.

ACh Sensitivity In Human-To-*Epipedobates* Mutants: High-Sensitivity Versus Low-Sensitivity nAChRs

The AA replacements in the human **LC**AI HS nAChR were able to perfectly maintain ACh sensitivity while decreasing epibatidine sensitivity (Fig. 2E and F). However, this pattern was slightly modified for human LS nAChRs, because even though the epibatidine sensitivity was greatly decreased, sensitivity to ACh also decreased, as the high-sensitivity component of the ACh curve was missing in these receptors, possibly because the S108C replacement altered the receptor stoichiometry (see above) (fig. S2A and S2B). The potential problem of decreased ACh sensitivity in LS receptors seems to have been solved in *Epipedobates* because they do not appear to form the LS nAChRs, at least in *Xenopus* oocytes. Thus, we speculate that the inability to form LS nAChRs could be an adaptation of *Epipedobates* as part of an imperfect solution to the cost of acetylcholine sensitivity incurred by the AA replacements that provide resistance.

Interestingly, all *Epipedobates* α4β2 nAChR (LCAI, **FS**AI, **L**SAI, and F**C**AI genotypes) were slightly more sensitive to ACh than human α4β2 nAChR (FSAI genotype), suggesting a slight but fundamental difference between mammalian and anuran nAChRs.

Fig. S1.

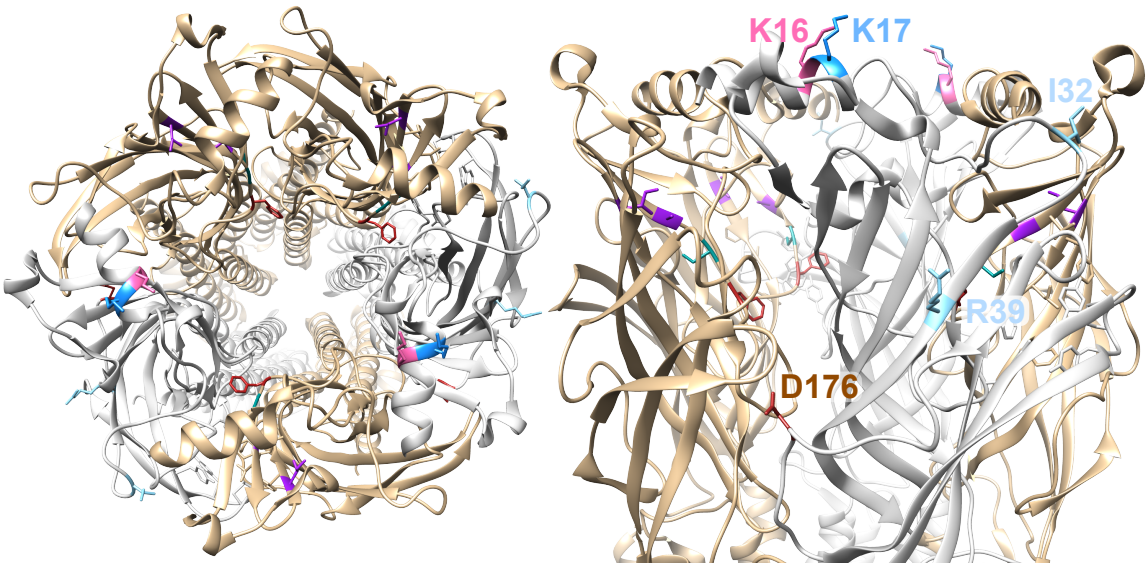

Fig. S1. AA replacements in α4 subunit of nicotinic acetylcholine receptor.
AA residues are labeled where AA replacements occur in *Epipedobates* (D176, brown), *Ameerega* (I32 and R39, light blue), *Oophaga* (K16, pink), both *Ameerega* and *Oophaga* (K17, blue). Alpha4 subunits are in gray and β2 subunits in gold.

Fig. S2.

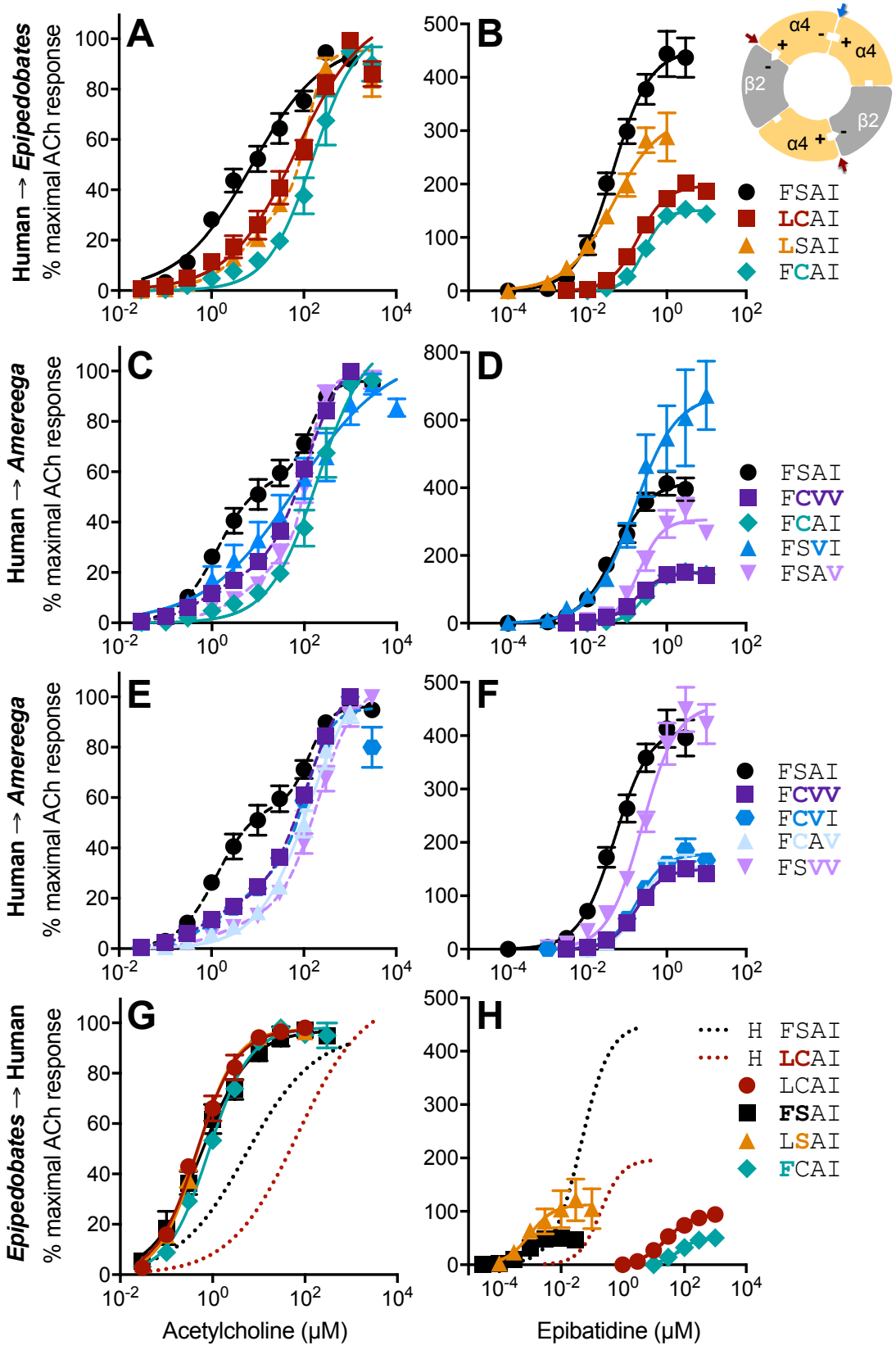
A
B
C
D
E
F
G
H
Human → Epipedobates
Human → Amereega
Epipedobates → Human
% maximal ACh response
Acetylcholine (μM)
Epibatidine (μM)
α4
β2
FSAI
LCAI
LSAI
FCAI
FCVV
FSVI
FSAV
FCVI
FCAV
FSVV
H FSAI
H LCAI
LCAI
FSAI
LSAI
FCAI

Fig. S2. ACh and epibatidine concentration-response curves in low-sensitivity α4β2 nAChR.

Left panels show responses to ACh and right panels show responses to epibatidine in nAChRs expressed in *Xenopus laevis* oocytes, recorded using two-electrode voltage clamp. (**A**, **B**) Human wild-type α4β2 nAChRs (FSAI genotype) and receptors containing the AA patterns identified in *Epipedobates* poison frogs (**LC**AI, **L**SAI and F**C**AI genotypes). (**C**, **D**) Human wild-type α4β2 nAChRs (FSAI genotype) and receptors containing the AA replacements identified in *Ameerega* (F**CVV**) along with the single mutants (F**C**AI, FS**V**I, FSA**V**). (**E**, **F**) Human wild-type α4β2 nAChRs (FSAI genotype) and receptors containing the AA replacements identified in *Ameerega* (F**CVV**) along with the double mutants (F**CV**I, F**CA**V, FS**VV**). (**G**, **H**) *Epipedobates* wild-type α4β2 nAChRs (LCAI genotype) and receptors containing the AA replacements identified in human (**FS**AI) along with the single mutants (**F**CAI, L**S**AI). Dotted lines (···) in panels G and H correspond to human FSAI and **LC**AI curves from A and B panels. Error bars not visible are smaller than the symbols. Data was fitted to either mono- (−) or biphasic (--) curves. Inset: schematic of LS α4β2 nAChR stoichiometry; ligand-binding sites indicated by red (high-sensitivity) and blue (low-sensitivity) arrows.

Fig. S3

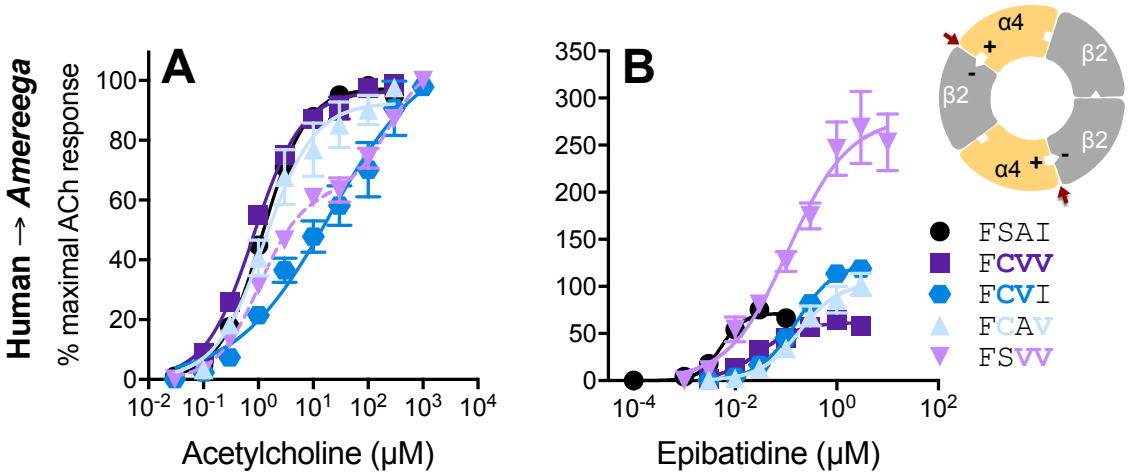

Fig. S3. ACh and epibatidine concentration-response curves in high-sensitivity α4β2 nAChR in human wild-type and double mutants.

Human wild-type α4β2 nAChRs (FSAI genotype) and receptors containing the AA replacements identified in *Ameerega* (F**CVV**) along with the double mutants (F**CV**I, F**CA**V, FS**VV**): responses to (**A**) ACh and (**B**) epibatidine. Inset: schematic of HS α4β2 nAChR subunit stoichiometry, with ligand binding sites indicated by arrows.

Fig. S4

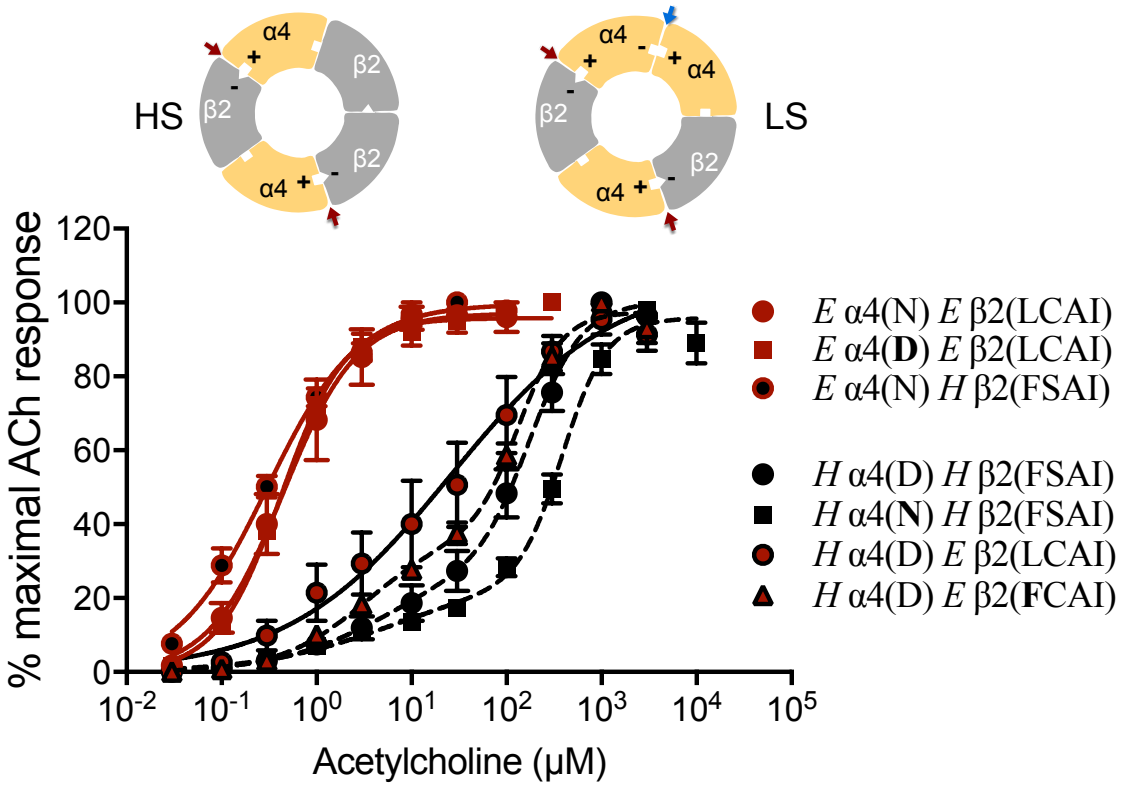

Fig. S4. ACh concentration-response curves (CRCs) in α4β2 nAChR composed of human subunits, *Epipedobates* subunits, and mixtures of the two (α:β ratio 7:1).

Human (*H*) wild-type α4β2 nAChRs [α4(D) and β2(FSAI) genotypes], *Epipedobates* (*E*) wild-type α4β2 nAChRs [α4(N) and β2(LCAI) genotypes], and combinations incorporating the mirror AA replacement patterns in α4 (**D** and **N**), as well as the *Epipedobates* β2(**F**CAI) genotype. Inset: schematic of α4β2 nAChR subunit stoichiometries, with ligand binding sites indicated by arrows.

Table S1. Specimen information.

Collection sites for sequenced individuals. TNHC-FS, Texas Natural History Collections Field Series; QCAZ, El Museo de Zoología de la Pontificia Universidad Católica del Ecuador; JCS, Juan Carlos Santos.

Genus	Species	Coordinates	Locality	Country	Museum Number (Field Series) / Sequence Read Archive	GenBank Accession No. (Chrnb2)	GenBank Accession No. (Chrna4)
Dendrobatid anurans							
Allobates	*femoralis*	0.040912N, −77.316382W	Lumbaquí	Ecuador	(JCS 2008)	MF580104	--
Allobates	*kingsburyi*	−2.81195S, −78.35395W	Plan Grande	Ecuador	(JCS 2008)	MF580102	--
Allobates	*talamancae*	1.175948N, −78.72983W	Tundaloma	Ecuador	(JCS 2008)	MF580089	MF580119
Allobates	*zaparo*	−1.91961S, −77.82273W	Río Pastaza	Ecuador	(JCS 2008)	MF580103	MF580111
Ameerega	*bilinguis*	−1.06214S, −77.600568W	Ahuano	Ecuador	(JCS 2008)	MF580088	--
Ameerega	*hahneli*	−1.59298S, −77.80866W	Canelos	Ecuador	(JCS 2008)	MF580085	MF580121
Ameerega	*parvula*	−2.81195S, −78.35395W	Gualaquiza	Ecuador	(JCS 2008)	MF580087	MF580118
Ameerega	*trivittata*		Leticia	Colombia	(RDT0163)	MF580086	--
Colostethus	*fugax*	−1.59298S, −77.80866W	Canelos	Ecuador	(JCS 2008)	MF580095	MF580120
Dendrobates (Andinobates)	*fulguritus*	5.611517N, −77.418186W	Termales	Colombia	ANDES-A2436 (RDT0128)	MF598759	--
Dendrobates (Excidobates)	*captivus*	−3.78255S, −78.74771W	Zumbi	Ecuador	(JCS 2008)	MF580096	--
Dendrobates (Oophaga)	*pumilio*	NA	Isla de Diamante	Nicaragua	LSUMZH-15103 (OMNH-33297)	MF598757	--
Dendrobates (Oophaga)	*sylvaticus*	−0.268356S, −79.12051W	Villa Hermosa	Ecuador	QCAZA58255 (RDT0035)	MF580098	MF598760
Dendrobates (Ranitomeya)	*ventrimaculatus*	NA	Leticia	Colombia	(RDT0164)	MF580107	--

Table S1 cont.							
Genus	**Species**	**Coordinates**	**Locality**	**Country**	**Museum Number (Field Series) / Sequence Read Archive**	**GenBank Accession No. (Chrnb2)**	**GenBank Accession No. (Chrna4)**
Dendrobatid anurans cont.							
Dendrobates	*truncatus*	4.19277N, −74.630953W	Melgar	Colombia	ANDES-A2427 (RDT0119)	MF580097	--
Epipedobates	*anthonyi*	−3.30756S, −79.77917W	El Progreso	Ecuador	(JCS 2008)	MF580094	MF580123
Epipedobates	*boulengeri*	0.10189N, −79.13724W	Arashá	Ecuador	(JCS 2008)	MF580092	MF580122
Epipedobates	*darwinwallacei*	−0.05539S, −78.78642W	Mindo	Ecuador	(JCS 2008)	MF580093	MF580110
Epipedobates	*machalilla*	−2.57390S, −79.35683W	Manta Real	Ecuador	(JCS 2008)	MF580091	MF580112
Epipedobates	*tricolor*	−1.37881S, −79.15575W	Chazo Juan	Ecuador	(JCS 2008)	MF580090	--
Hyloxalus	*italoi*	−1.60595S, −77.84275W	Canelos	Ecuador	(JCS 2008)	MF580083	MF580124
Hyloxalus	*jacobuspetersi*	−0.419S, −78.407W	Molinuco	Ecuador	(JCS 2008)	MF598758	--
Hyloxalus	*nexipus*	−2.74573S, −78.30503W	Río Negro	Ecuador	(JCS 2008)	MF580101	MF580125
Phyllobates	*aurotaenia*	3.985674N, −77.376574W	La Barra	Colombia	ANDES-A2456 (RDT0148)	MF580109	--
Phyllobates	*terribilis*	Black Jungle Terrarium Supply	NA	NA	purchased captive-bred individual	MF580108	--
Rheobates	*palmatus*	4.432908N, −73.920662W	Las Brisas	Colombia	ANDES-A2433 (RDT0125)	MF580106	--
Silverstoneia	*cf. gutturalis*	6.122443N −77.444037W	El Valle	Colombia	ANDES-A2444 (RDT0136)	MF580099	--
Silverstoneia	*cf. nubicola*	3.847596N −76.788457W	El Valle	Colombia	ANDES-A2466 (RDT0158)	MF580100	--
Bufo	*nebulifer*	30.31865N, −97.72620W	Austin	USA	TNHC-FS6877	MF580082	MF580113
Atelopus	*elegans*	NA	captive raised	Ecuador	(JCS 2008)	MF580084	MF580115

			from Esmeraldas Province				
Table S1 cont.							
Genus	**Species**	**Coordinates**	**Locality**	**Country**	**Museum Number (Field Series) / Sequence Read Archive**	**GenBank Accession No. (Chrnb2)**	**GenBank Accession No. (Chrna4)**
Non-dendrobatid anurans cont.							
Espadarana	*callistoma*	0.9123N, −78.5835W	Alto Tambo	Ecuador	(JCS 2008)	MF580080	MF580117
Gastrotheca	*sp.*	−3.40762S, −79.1345W	Ñamarin	Ecuador	(JCS 2008)	MF580105	MF580116
Boana	*picturata*	0.90775N, −78.59968W	El Placer	Ecuador	(JCS 2008)	MF580081	MF580114
Rana	*pipiens*	NA	NA	NA	SRR1185907, SRR1185248, SRR1185905, SRR1185669, SRR1185245	--	--
Xenopus	*tropicalis*				NA	BC136136.1	NM_001113843.1
Non-anuran outgroups							
Gallus	*gallus*				NA	AJ250362.1	--
Homo	*sapiens*				NA	NM_000748.2	NM_000744.6
Mus	*musculus*				NA	AF299083.1	--
Rattus	*norvegicus*				NA	AY574258.1	--

Table S2. Chrnb2 nucleotide alignment with AA residues and mutations of interest highlighted.

	106	108	110	118
Gallus gallus	ATGTACGAGGTCTCC**TTC**TAC**TCC**AAC**GCC**GTCATCTCCTACGACGGCAGC**ATC**TTCTGGCTGCCCCCCGCCATC			
Anolis carolinensis	ATGTACGAGGTGTCC**TTC**TAC**TCC**AAC**GCG**GTGGTCTCCTTCGACGGGAGC**ATC**TTCTGGCTCCCGCCGGCCATC			
Homo sapiens	ATGTACGAGGTGTCC**TTC**TAT**TCC**AAT**GCC**GTGGTCTCCTATGATGGCAGC**ATC**TTCTGGCTGCCGCCTGCCATC			
Rattus norvegicus	ATGTACGAAGTCTCC**TTC**TAT**TCC**AAT**GCT**GTGGTCTCCTATGATGGCAGC**ATC**TTTTGGCTACCACCTGCCATC			
Mus musculus	ATGTACGAAGTCTCC**TTC**TAT**TCC**AAT**GCT**GTGGTCTCCTATGATGGCAGC**ATC**TTTTGGCTACCGCCTGCCATC			
Xenopus tropicalis	ATGTACGAGGTGTCG**TTC**TAC**TCC**AAC**GCG**GTGGTGTCCCACGACGGCAGC**ATA**TTCTGGTTGCCCCCTGCCATA			
Rana pipiens	ATGTATGAGGTGTCC**TTC**TAC**TCC**AAC**GCG**GTTGTGTCGTACGATGGAAGC**ATC**TTTTGGTTGCCTCCAGCCATC			
Boana picturata	ATGTACGAGGTGTCC**TTC**TAC**TCC**AAC**GCG**GTGGTCTCCTATGACGGCAGC**ATC**TTCTGGCTTCCTCCCGCCATC			
Gastrotheca sp.	ATGTACGAGGTCTCC**TTC**TAC**TCC**AAC**GCG**GTGGTCTCCCACGACGGCAGC**ATC**TTCTGGCTGCCGCCCGCCATC			
Espadarana callistomma	ATGTACGAGGTTTCC**TTC**TAC**TCC**AAT**GCG**GTGGTCTCCTACGATGGGAGC**ATC**TTCTGGCTTCCTCCCGCCATC			
Atelopus elegans	ATGTACGAGGTTTCC**TTC**TAC**TCT**AAC**GCG**GTGGTCTCCTATGATGGAAGC**ATC**TTCTGGCTTCCTCCTGCTATC			
Bufo nebulifer	ATGTACGAGGTCTCC**TTC**TAC**TCT**AAC**GCG**GTGGTCTCCTACGATGGGAGC**ATC**TTCTGGCTTCCTCCCGCCATC			
Rheobates palmatus	ATGTACGAGGTCTCC**TTC**TAC**TCC**AAC**GCG**GTGGTCTCGCACGAYGGCAGC**ATC**TTCTGGCTGCCCCCCGCCATC			
Allobates talamancae	ATGTACGAGGTCTCC**TTC**TAC**TCA**AAC**GCG**GTGGTTTCGCATGACGGCAGC**ATC**TTCTGGTTGCCCCCCGCCATC			
Allobates kingsburyi	ATGTACGAGGTCTCA**TTC**TAC**TCG**AAT**GCG**GTGGTCTCGCATGACGGCAGC**ATC**TTCTGGCTACCCCCCGCCATC			
Allobates femoralis	ATGTACGAGGTCTCC**TTC**TAC**TCT**AAC**GCG**GTGGTCTCGCATGATGGTAGC**ATC**TTCTGGCTGCCCCCCGCCATC			
Allobates zaparo	ATGTACGAGGTCTCC**TTC**TAC**TCG**AAC**GCG**GTGGTTTCGCATGATGGTAGC**ATC**TTCTGGCTGCCCCCCGCCATC			
Hyloxalus italoi	ATGTATGAGGTCTCC**TTC**TAC**TCT**AAC**GCG**GTGGTCTCGCACGACGGCAGC**ATC**TTCTGGCTGCCCCCTGCCATC			
Hyloxalus jacobuspetersi	ATGTATGAGGTCTCC**TTC**TAC**TCT**AAT**GCA**GTGGTCTCGCACGACGGCAGC**ATC**TTCTGGCTGCCCCCCGCCATC			
Hyloxalus nexipus	ATGTATGAGGTCTCC**TTC**TAC**TCT**AAC**GCG**GTGGTCTCGCACGACGGTAGC**ATC**TTCTGGCTGCCCCCCGCCATC			
Phyllobates aurotaenia	ATGTATGAGGTCTCC**TTC**TAC**TCT**AAC**GCG**GTGGTCTCGCACGACGGCAGC**ATC**TTCTGGCTGCCCCCCGCCATC			
Phyllobates terribilis	ATGTATGAGGTCTCC**TTC**TAC**TCT**AAC**GCG**GTGGTCTCGCACGACGGCAGC**ATC**TTCTGGCTGCCCCCCGCCATC			
Dendrobates truncatus	ATGTATGAGGTCTCC**TTC**TAC**TCT**AAC**GCG**GTGGTCTCGCATGANGGCAGC**ATC**TTCTGGCTGCCACCCGCCATC			
Dendrobates sylvaticus	ATGTATGAGGTCTCC**TTC**TAC**TGT**AAT**GCG**GTGGTCTCGCATGATGGCAGC**ATC**TTCTGGCTGCCACCTGCCATC			
Dendrobates pumilio	ATGTATGAGGTCTCC**TTC**TAC**TGT**AAT**GCG**GTGGTCTCGCATGATGGCAGC**ATC**TTCTGGCTGCCACCCGCCATC			
Dendrobates captivus	ATGTATGAGGTCTCC**TTC**TAC**TCT**AAC**GCG**GTGGTCTCGCACGACGGCAGC**ATC**TTCTGGCTGCCACCCGCCATC			
Dendrobates fulguritus	ATGTACGAGGTCTCC**TTC**TAC**TCC**AAC**GCG**GTGGTCTCGCACGACGGCAGC**ATC**TTCTGGCTGCCCCCCGCCATC			
Dendrobates ventrimaculatus	ATGTATGAGGTCTCC**TTC**TAC**TCT**AAC**GCG**GTGGTCTCACACGACGGCAGC**ATC**TTCTGGCTGCCACCTGCCATT			
Colostethus fugax	ATGTACGAGGTCTCC**TTC**TAC**TCT**AAT**GCA**GTGGTTTCGCATGATGGCAGC**ATC**TTCTGGCTCCCCCCTGCCATC			
Ameerega parvula	ATGTACGAGGTCTCC**TTC**TAC**TGT**AAC**GTG**GTGGTTTCGCACGATGGCAGC**GTC**TTCTGGCTGCCCCCTGCCATC			
Ameerega bilinguis	ATGTACGAGGTCTCC**TTC**TAC**TGT**AAC**GTG**GTGGTTTCGCACGATGGCAGC**GTC**TTCTGGCTGCCCCCTGCCATC			
Ameerega hahneli	ATGTACGAGGTCTCC**TTC**TAC**TGT**AAC**GTG**GTGGTTTCGCACGACGGCAGC**GTC**TTCTGGCTGCCCCCCGCCATC			
Ameerega trivittata	ATGTACGAGGTCTCC**TTC**TAC**TGT**AAC**GTG**GTGGTTTCACACGATGGCAGC**GTC**TTCTGGCTGCCCCCTGCCATC			
Silverstoneia cf. nubicola	ATGTATGAGGTCTCC**TTC**TAC**TCT**AAT**GCA**GTGGTTTCACATGACGGCAGC**ATC**TTCTGGCTGCCCCCCGCCATC			
Silverstoneia cf. gutturalis	ATGTATGAGGTCTCC**TTC**TAC**TCT**AAC**GCA**GTGGTTTCACATGACGGCAGC**ATC**TTCTGGCTGCCCCCCGCCATC			
Epipedobates boulengeri	ATGTATGAGGTCTCC**CTC**TAC**TGT**AAT**GCA**GTGGTTTCACATGACGGCAGC**ATC**TTCTGGCTGCCCCCCGCCATC			
Epipedobates darwinwallacei	ATGTATGAGGTCTCC**CTC**TAC**TGT**AAT**GCA**GTGGTTTCACATGACGGCAGC**ATC**TTCTGGCTGCCCCCCGCCATC			
Epipedobates anthonyi	ATGTATGAGGTCTCC**CTC**TAC**TGT**AAT**GCA**GTGGTTTCACATGACGGCAGC**ATC**TTCTGGCTGCCCCCCGCCATC			
Epipedobates machalilla	ATGTATGAGGTCTCC**CTC**TAC**TGT**AAT**GCA**GTGGTTTCACATGACGGCAGC**ATC**TTCTGGCTGCCCCCCGCCATC			
Epipedobates tricolor	ATGTATGAGGTCTCC**CTC**TAC**TGT**AAT**GCA**GTGGTATCACATGATGGCAGC**ATC**TTCTGGCTGCCCCCCGCCATC			

Table S3. Chrna4 AA alignment with AA residues of interest highlighted.

Amino acid replacements (highlighted) in chrna4 unique to *Epipedobates, Ameerega,* or *Dendrobates* (*Oophaga*). AA residue numbers are indicated above the alignment. Additional AA differences between human and *Epipedobates* near position 176 are underlined.

	17	32	39	…	176
Homo sapiens	HAEERLLKKLFSGYNKWSRPVANISDVVLVRFGLSIAQL				DKAKIDLVNMHSRVDQLDFWESGEWVIVDAVGTYNTRKYECCAEIYPDI
Xenopus tropicalis	HAEERLLKGLFSGYNKWSRPVANISDAVMVRFGLSIAQL				DRAKIDLISMHSHVDQLDYWESGEWVIVNAVGNYNIKKYECCTEIYSDI
Boana picturata	HAEERLLKKLFKEYNKWSRPVANISDAVLVRFGLSIAQL				DRAKIDLISMHNHVDQLDYWESGEWVIVNAVGNYNIKKYECCTEIYSDI
Espadarana callistomma	HAEERLLKKLFMGYNKWSRPVANISDAVLVRFGLSIAQL				DRAKIDLISMHNHVDQLDYWESGEWVIVNAVGNYNIKKYECCTEIYSDI
Gastrotheca sp.	HAEERLLKKLFMEYNKWSRPVANISDAVLVRFGLSIAQL				DRAKIDLISMHNHVDQLDYWESGEWVIVNAVGNYNIKKYECCTEIYSDI
Bufo nebulifer	HAEERLLKKLFMAYNKWSRPVANISDAVLVRFGLSIAQL				DRAKIDLISMHNHVDQLDYWESGEWVIVNAVGNYNIKKYECCTEIYSDI
Atelopus elegans	HAEERLLKKLFMAYNKWSRPVANISDAVLVRFGLSIAQL				DRAKIDLISMHNHVDQLDYWESGEWVIVNAVGNYNIKKYECCTEIYSDI
Allobates zaparo	HAEERLLKKLFLGYNKWSRPVANISDAVLVRFGLSIAQL				DRAKIDLISMHSHVDQLDYWESGEWVIVNAVGNYNIKKYECCTEIYSDI
Allobates talamancae	HAEERLLKKLFLGYNKWSRPVANISDAVLVRFGLSIAQL				DRAKIDLISMHSHVDQLDYWESGEWVIVNAVGNYNIKKYECCTEIYSDI
Hyloxalus italoi	HAEERLLKKLFMGYNKWSRPVANISDAVLVRFGLSIAQL				DRAKIDLISMHSHVDQLDYWESGEWVIVNAVGNYNIKKYECCTEIYSDI
Hyloxalus nexipus	HAEERLLKKLFMGYNKWSRPVANISDAVLVRFGLSIAQL				DKAKIDLISMHSHVDQLDYWESGEWVIVNAVGNYNIKKYECCTEIYSDI
Dendrobates sylvaticus	HAEERLL**QE**LFMGYNKWSRPVANISDAVLVRFGLSIAQL				DKAKIDLISMHNHVDQLDYWESGEWVIVNAVGNYNIKKYECCTEIYSDI
Colosthethus fugax	HAEERLLKKLFMGYNKWSRPVANISDAVLVRFGLSIAQL				DKAKIDLISMHSHVDQLDYWESGEWVIVNAVGNYNIKKYECCTEIYSDI
Ameerega parvula	HAEERLLK**N**LFMGYNKWSRPVAN**T**SDAVLV**L**FGLSIAQL				DKAKIDLISMHNHVDQLDYWESGEWVIVNAVGNYNIKKYECCTEIYSDI
Ameerega bilinguis	HAEERLLK**N**LFMGYNKWSRPVAN**T**SDAVLV**L**FGLSIAQL				DKAKIDLISMHNHVDQLDYWESGEWVIVNAVGNYNIKKYECCTEIYSDI
Ameerega hahneli	HAEERLLK**N**LFMGYNKWSRPVAN**T**SDAVLV**L**FGLSIAQL				DKAKIDLISMHNHVDQLDYWESGEWVIVNAVGNYNIKKYECCAEIYSDI
Phyllobates terribilis	----------				DRAKIDLISMHSHVDQLDYWESGEWVIVNAVGNYNIKKYECCTEIYSDI
Epipedobates anthonyi	HAEERLLKKLFMGYNKWSRPVANISDAVLVRFGLSIAQL				DKAKIDLISMHSHVDQL**N**YWESGEWVIVNAVGNYNIKKYECCTEIYSDI
Epipedobates tricolor	----------				DKAKIDLISMHSHVDQL**N**YWESGEWVIVNAVGNYNIKKYE---------
Epipedobates boulengeri	HAEERLLKKLFMGYNKWSRPVANISDAVLVRFGLAIAQL				DRAKIDLISMHSHVDQL**N**YWESGEWVIVNAVGNYNIKKYECCTEIYSDI

Table S4. Accession numbers for sequences used in Fig. 1 phylogeny.

GenBank accession numbers for genes used to infer the reference phylogeny for Figure 1. Photographs in the figure are of individuals QCAZA58255 (*D.* [*O.*] *sylvaticus*), QCAZA58327 (*A. hahneli*), QCAZA58321 (*A. bilinguis*), QCAZA58301 (*E. tricolor*), and QCAZA53675 (*E. anthonyi*).

Genus	**Species**	**12S-16S-ND2**	**CYTB**
Gallus	*gallus*	X52392	X52392
Homo	*sapiens*	KJ446330	KJ446330
Rattus	*norvegicus*	KF011917	KF011917
Mus	*musculus*	AB042432	AB042432
Xenopus	*tropicalis*	AY789013	AY789013
Rana	*yavapaiensis*	DQ283272 GU184243	GU184212
Boana	*picturata*	AY326055	--
Mantella	*aurantiaca*	DQ283035	AY723593
Gastrotheca	*sp.*	DQ679247 KJ489515	--
Espadarana	*callistomma*	EU663340, EU663076, EU662981	--
Atelopus	*elegans*	MF619959	MF598761
Bufo	*nebulifer*	HQ290945	HQ290525
Rheobates	*palmatus*	HQ290967	HQ290545
Allobates	*talamancae*	HQ290974	HQ290552
Allobates	*kingsburyi*	HQ290963	HQ290541
Allobates	*femoralis*	HQ290951	HQ290531
Allobates	*zaparo*	HQ291003	HQ290580
Hyloxalus	*italoi*	HQ290972	HQ290550
Hyloxalus	*jacobspetersi*	MF619960	MF598762
Hyloxalus	*nexipus*	HQ290965	HQ290543
Phyllobates	*aurotaenia*	HQ291005	HQ290582
Phyllobates	*terribilis*	HQ291006	HQ290583
Dendrobates	*truncatus*	HQ290992	HQ290569
Dendrobates	*sylvaticus*	HQ290990	HQ290567
Dendrobates	*pumilio*	HQ290988	HQ290565
Dendrobates	*captivus*	HQ290982	HQ290559
Dendrobates	*fulguritus*	HQ290989	HQ290566
Dendrobates	*ventrimaculatus*	HQ290979	HQ290556
Colostethus	*fugax*	HQ290958	HQ290538
Ameerega	*parvula*	HQ290999	HQ290576
Ameerega	*bilinguis*	HQ290996	HQ290573
Ameerega	*hahneli*	HQ290998	HQ290575
Ameerega	*trivittata*	HQ291002	HQ290579
Silverstoneia	*nubicola*	HQ290966	HQ290544
Silverstoneia	*flotator*	HQ290957	HQ290537

Table S4 cont.			
Genus	**Species**	**12S-16S-ND2**	**CYTB**
Epipedobates	*anthonyi*	HQ290995	HQ290572
Epipedobates	*tricolor*	HQ291001	HQ290578
Epipedobates	*machalilla*	HQ290964	HQ290542
Epipedobates	*boulengeri*	HQ290997	HQ290574
Epipedobates	*darwinwallacei*	HQ291000	HQ290577

Table S5. Concentration-response curve parameters from human α4β2 nAChR containing β2 subunits mutated to have *Epipedobates* amino acids.

Please note that the single mutant L**C**AI also corresponds to the *Dendrobates* (*Oophaga*) AA replacement pattern. EC_{50}, effective concentration 50; *nH*, Hill coefficient; *n*, number of oocytes; % Max Resp, % of maximal ACh responses. Data is presented as mean (95% confidence interval) or mean ± SEM. 1:3 and 3:1 indicate the α4:β2 cRNA ratio injected. Two values are given where the CRC is biphasic (one high and one low sensitivity).

Ligand	Genotype	1:3				3:1			
		EC_{50} (μM)	% Maximal Response	n_H	*n*	EC_{50} (μM)	% Maximal Response	n_H	*n*
ACh	FSAI	1.3 (1.1 − 1.5)	99 ± 2	1.1 ± 0.1	7	7.4 (4.2 − 13)	99 ± 5	0.6 ± 0.1	9
	LCAI	1.4 (1.0 − 2.2)	97 ± 4	0.9 ± 0.1	6	68 (32 − 147)	111 ± 9	0.6 ± 0.1	6
	LSAI	1.1 (1.0 − 1.3)	98 ± 2	1.2 ± 0.1	6	8.7 (0.8 − 111) 120 (96 − 149)	42 ± 21 53 ± 19	0.8 ± 0.3 2.5 ± 1.0	6
	F**C**AI	3.1 (0.4 − 26) 136 (92 − 202)	33 ± 12 54 ± 12	0.9 ± 0.6 3.1 ± 1.5	6	155 (92 − 263)	105 ±8	0.9 ± 0.1	4
Epibatidine	FSAI	5.2 (3.3 − 8.3)	78 ± 6	1.8 ± 0.6	9	45 (29 − 68)	452 ± 23	0.9 ± 0.1	9
	LCAI	88 (60 − 128)	79 ± 3	0.9 ± 0.1	6	190 (157 − 231)	197 ± 5	1.2 ± 0.1	4
	LSAI	4.1 (3.0 − 5.7)	55 ± 3	2.1 ± 0.6	6	44 (16 − 120)	327 ± 41	0.7 ± 0.2	6
	F**C**AI	256 (205 − 321)	137 ± 4	1.4 ± 0.2	4	267 (208 − 343)	151 ± 6	1.7 ± 0.3	5

Table S6. Concentration-response curve parameters from human α4β2 nAChR containing β2 subunits mutated to have *Ameerega* amino acids.

Please note that the single mutant L**C**AI also corresponds to the *Dendrobates* (*Oophaga*) AA replacement pattern. EC_{50}, effective concentration 50; *nH*, Hill coefficient; *n*, number of oocytes; % Max Resp, % of maximal ACh response. Data is presented as mean (95% confidence interval) or mean ± SEM. 1:3 and 3:1 indicate the α4:β2 cRNA ratio injected. Two values are given where the CRC is biphasic (one high and one low sensitivity).

Ligand	Genotype	1:3				3:1			
		EC_{50} (μM)	% Maximal Response	n_H	*n*	EC_{50} (μM)	% Maximal Response	n_H	*n*
ACh	FSAI	1.2 (1.1 − 1.3)	98 ± 1	1.1 ± 0.1	13	1.3 (0.7 − 2.5) 131 (75 − 229)	58 ± 7 38 ± 9	1.0 ± 0.2 1.9 ± 0.9	18
	F**C**V**V**	0.8 (0.7 − 0.9)	96 ± 1	1.0 ± 0.1	6	0.6 (0.1 − 4.3) 110 (80 − 151)	18 ± 8 91 ± 12	1.0 ± 0.5 1.0 ± 0.2	5
	F**C**V**I**	20 (7 − 62)	110 ± 11	0.5 ± 0.1	6	3.7 (0.1 − 115) 117 (79 − 172)	36 ± 21 60 ± 21	0.7 ± 0.3 1.7 ± 0.5	6
	F**C**A**V**	1.3 (0.8 − 2.0)	93 ± 4	1.0 ± 0.2	6	142 (70 − 287)	117 ± 12	0.8 ± 0.2	6
	FS**V**V	1.04 (0.7 − 1.7) 244 (102 − 582)	63 ± 6 44 ± 15	0.5 ± 0.1	5	1.7 (0 − 136) 201 (140 − 290)	12 ± 11 93 ± 14	0.9 ± 0.8 1.1 ± 0.2	4
	F**C**AI	3.2 (0.3 − 35) 163 (106 − 252)	33 ± 13 62 ± 14	0.6 ± 0.1	6	196 (107 − 359)	114 ± 10	0.8 ± 0.1	6
	FS**V**I	1.1 (1.0 − 1.3)	97 ± 1	1.1 ± 0.1	4	69 (15 − 320)	108 ± 14	0.4 ± 0.1	6
	FSA**V**	8 (0.6 − 118) 124 (89 − 171)	34 ± 18 57 ± 17	1.0 ± 0.1 4.1 ± 3.3	5	17 (0 − 11,000) 123 (92 − 162)	42 ± 52 58 ± 44	0.7 ± 0.4 2.7 ± 2.2	5
Epibatidine	FSAI	5.3 (3.6 − 7.7)	71 ± 5	1.9 ± 0.5	17	49 (33 − 74)	417 ± 21	1.0 ± 0.2	14
	F**C**V**V**	31 (19 − 51)	62 ± 3	1.1 ± 0.2	6	172 (139 − 212)	150 ± 4	1.3 ± 0.2	6
	F**C**V**I**	162 (101 − 259)	125 ± 9	1.2 ± 0.2	6	181 (128 − 256)	178 ± 8	1.3 ± 0.2	5
	F**C**A**V**	184 (94 − 358)	104 ± 11	1.1 ± 0.3	5	171 (120 − 245)	154 ± 8	1.5 ± 0.4	5
	FS**V**V	113 (50 to 253)	279 ± 23	0.7 ± 0.2	4	237 (156 − 360)	458 ± 25	1.0 ± 0.2	5
	F**C**AI	256 (205 − 321)	137 ± 4	1.4 ± 0.2	4	267 (208 − 343)	151 ± 6	1.7 ± 0.3	5
	FS**V**I	6.5 (4.3 − 10)	71 ± 6	2.6 ± 0.9	6	150 (56 − 405)	676 ± 80	0.8 ± 0.2	5
	FSA**V**	395 (290 − 537)	184 ± 9	1.2 ± 0.2	5	201 (130 − 310)	306 ± 19	1.5 ± 0.4	5

Table S7. Concentration-response curve parameters from *Epipedobates* α4β2 nAChR containing β2 nAChR mutated to have human amino acids.

EC50, effective concentration 50; *nH*, Hill coefficient; *n*, number of oocytes; % Max Resp, % of maximal ACh response. Data is presented as mean (95% confidence interval) or mean ± SEM. 1:7 and 7:1 indicate the α4:β2 cRNA ratio injected.

Ligand	Genotype	1:7				7:1			
		EC_{50} (μM)	% Maximal Response	n_H	*n*	EC_{50} (μM)	% Maximal Response	n_H	*n*
ACh	LCAI	0.42 (0.38 − 0.48)	98 ± 1	1.2 ± 0.1		0.45 (0.36 − 0.57)	98 ± 2	1.0 ± 0.1	13
	FSAI	0.44 (0.34 − 0.57)	95 ± 3	1.2 ± 0.1	6	0.58 (0.41 − 0.84)	97 ± 3	0.8 ± 0.1	5
	FCAI	0.87 (0.71 − 1.1)	98 ± 2	1.1 ± 0.1	5	0.83 (0.71 − 0.97)	98 ± 2	1.0 ± 0.1	6
	L**S**AI	0.51 (0.36 − 0.76)	98 ± 4	1.0 ± 0.1	5	0.47 (0.40 − 0.55)	98 ± 2	1.1 ± 0.1	5
Epibatidine	LCAI	15 (10 − 22)	30 ± 2	1.5 ± 0.3	6	25 (11 − 210)	94 ± 12	1.1 ± 0.4	8
	FSAI	0.34 (0.28 − 0.48)	70 ± 4	4.0 ± 4.8	5	0.71 (0.59 − 0.84)	50 ± 1	1.8 ± 0.2	7
	FCAI	47 (37 − 60)	30 ± 1	1.2 ± 0.1	4	67 (34 − 236)	51 ± 6	1.3 ± 0.5	5
	L**S**AI	0.6 (0.4 − 1.0)	55 ± 5	1.6 ± 0.4	4	0.9 (0.59 − 0.84)	115 ± 17	1.3 ± 0.8	8

Table S8. Concentration-response curve parameters from α4β2 nAChR composed of human and *Epipedobates* subunits (α4:β2 cRNA ratio 7:1).

Human (*H*) wild-type α4β2 nAChRs [α4(D) and β2(FSAI) genotypes], *Epipedobates* (E) wild-type α4β2 nAChRs [α4(N) and β2(LCAI) genotypes], and combinations incorporating the mirror AA replacement patterns in α4 (**D** and **N**), as well as the *Epipedobates* β2(**F**CAI) genotype. EC_{50}, effective concentration 50; *nH*, Hill coefficient; *n*, number of oocytes; % Max Resp, % of maximal ACh response; *H*, human; *E*, *Epipedobates*. Data is presented as mean (95% confidence interval) or mean ± SEM. Two values are given where the CRC is biphasic (one high and one low sensitivity).

Ligand	Receptor (Genotype)	7:1			
		EC_{50} (μM)	% Maximal Response	n_H	*n*
ACh	*E* α4(N) *E* β2(LCAI)	0.45 (0.31 to 0.67)	97 ± 4	1.1 ± 0.2	4
	E α4(**D**) *E* β2(LCAI)	0.42 (0.37 to 0.48)	96 ± 1	1.3 ± 0.1	5
	E α4(N) *H* β2(FSAI)	0.3 (0.25 to 0.37)	100 ± 2	0.9 ± 0.1	6
	H α4(D) *H* β2(FSAI)	5.4 (0.21 to 191) 178 (109 to 330)	30 ± 29 70 ± 30	0.8 ± 0.5 1.6 ± 0.6	3
	H α4(**N**) *H* β2(FSAI)	6.0 (0.5 to 147) 387 (303 to 492)	25 ± 13 71 ± 13	0.6 ± 0.3 1.9 ± 0.4	6
	H α4(D) *E* β2(LCAI)	26 (9.3 to 176)	107 ± 12	0.5 ± 0.1	5
	H α4(D) *E* β2(**F**CAI)	3.2 (1.1 to 17) 134 (97 to 186)	38 ± 9 60 ± 9	1.0 ± 0.3 1.9 ± 0.4	4

Table S9. Statistical comparisons of the effect of receptor stoichiometry and genotype on response to epibatidine (logEC_{50}) of Human-to-*Epipedobates* mutated nAChRs. HS: high sensitivity (1:7 ratio); LS: low sensitivity (7:1 ratio).

A. Two-way ANOVA

Source of Variation	% of total variation	SS (Type III)	DF	MS	F (DFn, DFd)	*P* value
Interaction	4.193	13.84	3	4.612	F (3, 337) = 8.217	<0.001
Stoichiometry (HS vs. LS)	8.011	26.44	1	26.44	F (1, 337) = 47.10	<0.001
Receptor Genotype	30.48	100.6	3	33.53	F (3, 337) = 59.73	<0.001
Residual		189.2	337	0.5613		

B. Tukey's multiple comparisons test.

Receptor Comparison	Mean Difference ± SE	q	Adjusted *P* Value
HS:FSAI vs. HS:**L**CAI	−1.227 ± 0.151	11.52	**<0.001**
HS:FSAI vs. HS:F**C**AI	−1.693 ± 0.172	13.89	**<0.001**
HS:FSAI vs. HS:**L**SAI	0.100 ± 0.166	0.853	0.999
HS:FSAI vs. LS:FSAI	−0.933 ± 0.136	9.703	**<0.001**
HS:FSAI vs. LS:**L**CAI	−1.563 ± 0.172	12.83	**<0.001**
HS:FSAI vs. LS:F**C**AI	−1.710 ± 0.167	14.45	**<0.001**
HS:FSAI vs. LS:**L**SAI	−0.929 ± 0.154	8.522	**<0.001**
HS:**L**CAI vs. HS:F**C**AI	−0.466 ± 0.174	3.776	0.136
HS:**L**CAI vs. HS:**L**SAI	1.327 ± 0.168	11.17	**<0.001**
HS:**L**CAI vs. LS:FSAI	0.294 ± 0.139	3.002	0.402
HS:**L**CAI vs. LS:**L**CAI	−0.336 ± 0.174	2.728	0.532
HS:**L**CAI vs. LS:F**C**AI	−0.483 ± 0.169	4.033	0.086
HS:**L**CAI vs. LS:**L**SAI	0.298 ± 0.156	2.695	0.548
HS:F**C**AI vs. HS:**L**SAI	1.793 ± 0.188	13.51	**<0.001**
HS:F**C**AI vs. LS:FSAI	0.760 ± 0.162	6.637	**<0.001**
HS:F**C**AI vs. LS:**L**CAI	0.129 ± 0.194	0.945	0.998
HS:F**C**AI vs. LS:F**C**AI	−0.018 ± 0.189	0.132	>0.999
HS:F**C**AI vs. LS:**L**SAI	0.764 ± 0.177	6.087	**<0.001**
HS:**L**SAI vs. LS:FSAI	−1.033 ± 0.155	9.431	**<0.001**
HS:**L**SAI vs. LS:**L**CAI	−1.663 ± 0.188	12.53	**<0.001**
HS:**L**SAI vs. LS:F**C**AI	−1.810 ± 0.183	13.98	**<0.001**
HS:**L**SAI vs. LS:**L**SAI	−1.029 ± 0.171	8.506	**<0.001**
LS:FSAI vs. LS:**L**CAI	−0.630 ± 0.162	5.508	**0.003**
LS:FSAI vs. LS:F**C**AI	−0.777 ± 0.157	7.023	**<0.001**
LS:FSAI vs. LS:**L**SAI	0.004 ± 0.142	0.040	>0.999
LS:**L**CAI vs. LS:F**C**AI	−0.147 ± 0.189	1.098	0.994
LS:**L**CAI vs. LS:**L**SAI	0.634 ± 0.177	5.057	**0.009**
LS:F**C**AI vs. LS:**L**SAI	0.781 ± 0.173	6.403	**<0.001**

Table S10. Statistical comparisons of the effect of receptor stoichiometry and genotype on response to epibatidine (maximal current) of Human-to-*Epipedobates* mutated nAChRs. HS: high sensitivity (1:7 ratio); LS: low sensitivity (7:1 ratio).

A. Two-way ANOVA

Source of Variation	% of total variation	SS (Type III)	DF	MS	F (DFn, DFd)	*P* value
Interaction	12.93	1508445	3	502815	F (3, 337) = 26.62	<0.001
Stoichiometry (HS vs. LS)	25.56	2982874	1	2982874	F (1, 337) = 157.9	<0.001
Receptor Genotype	6.978	814334	3	271445	F (3, 337) = 14.37	<0.001
Residual		6365012	337	18887		

B. Tukey's multiple comparisons test.

Receptor Comparison	Mean Difference ± SE	q	Adjusted *P* Value
HS:FSAI vs. HS:**L**CAI	−0.990 ± 27.64	0.051	>0.999
HS:FSAI vs. HS:F**C**AI	−58.72 ± 31.62	2.626	0.582
HS:FSAI vs. HS:**L**SAI	22.96 ± 30.43	1.067	0.995
HS:FSAI vs. LS:FSAI	−373.9 ± 24.94	21.20	**<0.001**
HS:FSAI vs. LS:**L**CAI	−119.2 ± 31.62	5.332	**0.005**
HS:FSAI vs. LS:F**C**AI	−72.82 ± 30.70	3.354	0.259
HS:FSAI vs. LS:**L**SAI	−248.7 ± 28.28	12.44	**<0.001**
HS:**L**CAI vs. HS:F**C**AI	−57.73 ± 31.99	2.553	0.617
HS:**L**CAI vs. HS:**L**SAI	23.95 ± 30.81	1.099	0.994
HS:**L**CAI vs. LS:FSAI	−372.9 ± 25.40	20.76	**<0.001**
HS:**L**CAI vs. LS:**L**CAI	−118.2 ± 31.99	5.227	**0.006**
HS:**L**CAI vs. LS:F**C**AI	−71.83 ± 31.08	3.269	0.291
HS:**L**CAI vs. LS:**L**SAI	−247.7 ± 28.68	12.21	**<0.001**
HS:F**C**AI vs. HS:**L**SAI	81.68 ± 34.43	3.355	0.258
HS:F**C**AI vs. LS:FSAI	−315.2 ± 29.69	15.01	**<0.001**
HS:F**C**AI vs. LS:**L**CAI	−60.50 ± 35.48	2.411	0.684
HS:F**C**AI vs. LS:F**C**AI	−14.10 ± 34.67	0.575	>0.999
HS:F**C**AI vs. LS:**L**SAI	−190.0 ± 32.54	8.258	**<0.001**
HS:**L**SAI vs. LS:FSAI	−396.9 ± 28.41	19.75	**<0.001**
HS:**L**SAI vs. LS:**L**CAI	−142.2 ± 34.43	5.841	**0.001**
HS:**L**SAI vs. LS:F**C**AI	−95.78 ± 33.58	4.033	0.086
HS:**L**SAI vs. LS:**L**SAI	−271.7 ± 31.38	12.24	**<0.001**
LS:FSAI vs. LS:**L**CAI	254.7 ± 29.69	12.13	**<0.001**
LS:FSAI vs. LS:F**C**AI	301.1 ± 28.71	14.83	**<0.001**
LS:FSAI vs. LS:**L**SAI	125.2 ± 26.10	6.785	**<0.001**
LS:**L**CAI vs. LS:F**C**AI	46.40 ± 34.67	1.893	0.884
LS:**L**CAI vs. LS:**L**SAI	−129.5 ± 32.54	5.628	**0.002**
LS:F**C**AI vs. LS:**L**SAI	−175.9 ± 31.65	7.860	**<0.001**

Table S11. Statistical comparisons of the effect of receptor stoichiometry and genotype on response to epibatidine (logEC_{50}) of Human-to-*Ameerega* mutated nAChRs. HS: high sensitivity (1:3 ratio); LS: low sensitivity (3:1 ratio).

A. Two-way ANOVA

Source of Variation	% of total variation	SS (Type III)	DF	MS	F (DFn, DFd)	*P* value
Interaction	7.593	45.47	7	6.496	F (7, 719) = 11.23	<0.001
Stoichiometry (HS vs. LS)	4.035	24.16	1	24.16	F (1, 719) = 41.79	<0.001
Receptor Genotype	18.95	113.5	7	16.21	F (7, 719) = 28.04	<0.001
Residual		415.7	719	0.579		

B. Tukeys's multiple comparisons test.

Receptor Comparison	Mean Difference ± SE	q	Adjusted *P* Value
HS:FSAI vs. HS:F**C**V**V**	−0.774 ± 0.143	7.683	**<0.001**
HS:FSAI vs. HS:F**C**V**I**	−1.485 ± 0.143	14.75	**<0.001**
HS:FSAI vs. HS:F**C**A**V**	−1.541 ± 0.153	14.26	**<0.001**
HS:FSAI vs. HS:FS**V**V	−1.330 ± 0.155	12.17	**<0.001**
HS:FSAI vs. HS:F**C**AI	−1.686 ± 0.159	15.04	**<0.001**
HS:FSAI vs. HS:FS**V**I	−0.093 ± 0.151	0.870	>0.999
HS:FSAI vs. HS:FSA**V**	−1.873 ± 0.155	17.13	**<0.001**
HS:FSAI vs. LS:FSAI	−0.968 ± 0.104	13.21	**<0.001**
HS:FSAI vs. LS:F**C**V**V**	−1.512 ± 0.136	15.76	**<0.001**
HS:FSAI vs. LS:F**C**V**I**	−1.534 ± 0.139	15.62	**<0.001**
HS:FSAI vs. LS:F**C**A**V**	−1.511 ± 0.153	13.98	**<0.001**
HS:FSAI vs. LS:FS**V**V	−1.651 ± 0.139	16.81	**<0.001**
HS:FSAI vs. LS:F**C**AI	−1.703 ± 0.153	15.76	**<0.001**
HS:FSAI vs. LS:FS**V**I	−1.453 ± 0.136	15.15	**<0.001**
HS:FSAI vs. LS:FSA**V**	−1.579 ± 0.153	14.61	**<0.001**
HS:F**C**V**V** vs. HS:F**C**V**I**	−0.711 ± 0.170	5.917	**0.003**
HS:F**C**V**V** vs. HS:F**C**A**V**	−0.767 ± 0.179	6.068	**0.002**
HS:F**C**V**V** vs. HS:FS**V**V	−0.556 ± 0.180	4.363	0.138
HS:F**C**V**V** vs. HS:F**C**AI	−0.912 ± 0.184	7.020	**<0.001**
HS:F**C**V**V** vs. HS:FS**V**I	0.681 ± 0.177	5.430	**0.013**
HS:F**C**V**V** vs. HS:FSA**V**	−1.099 ± 0.180	8.621	**<0.001**
HS:F**C**V**V** vs. LS:FSAI	−0.194 ± 0.139	1.972	0.991
HS:F**C**V**V** vs. LS:F**C**V**V**	−0.738 ± 0.164	6.349	**<0.001**
HS:F**C**V**V** vs. LS:F**C**V**I**	−0.760 ± 0.167	6.430	**<0.001**
HS:F**C**V**V** vs. LS:F**C**A**V**	−0.737 ± 0.179	5.829	**0.004**
HS:F**C**V**V** vs. LS:FS**V**V	−0.877 ± 0.167	7.427	**<0.001**
HS:F**C**V**V** vs. LS:F**C**AI	−0.929 ± 0.179	7.349	**<0.001**
HS:F**C**V**V** vs. LS:FS**V**I	−0.679 ± 0.164	5.845	**0.004**
HS:F**C**V**V** vs. LS:FSA**V**	−0.805 ± 0.179	6.368	**<0.001**
HS:F**C**V**I** vs. HS:F**C**A**V**	−0.056 ± 0.179	0.442	>0.999
HS:F**C**V**I** vs. HS:FS**V**V	0.155 ± 0.180	1.215	>0.999

Table S11B cont.			
Receptor Comparison	**Mean Difference ± SE**	**q**	**Adjusted *P* Value**
HS:F**C**V**V**I vs. HS:F**C**A**V**I	−0.200 ± 0.184	1.542	>0.999
HS:F**C**V**V**I vs. HS:FS**V**VI	1.392 ± 0.177	11.10	**<0.001**
HS:F**C**V**V**I vs. HS:FSA**V**V	−0.388 ± 0.180	3.043	0.731
HS:F**C**V**V**I vs. LS:FSA**V**I	0.517 ± 0.139	5.259	0.020
HS:F**C**V**V**I vs. LS:F**C**V**V**V	−0.027 ± 0.164	0.229	>0.999
HS:F**C**V**V**I vs. LS:F**C**V**V**I	−0.048 ± 0.167	0.407	>0.999
HS:F**C**V**V**I vs. LS:F**C**A**V**V	−0.026 ± 0.179	0.203	>0.999
HS:F**C**V**V**I vs. LS:FS**V**V**V**	−0.166 ± 0.167	1.404	>0.999
HS:F**C**V**V**I vs. LS:F**C**A**V**I	−0.218 ± 0.179	1.722	0.998
HS:F**C**V**V**I vs. LS:FS**V**VI	0.032 ± 0.164	0.275	>0.999
HS:F**C**V**V**I vs. LS:FSA**V**V	−0.094 ± 0.179	0.742	>0.999
HS:F**C**A**V**V vs. HS:FS**V**V**V**	0.211 ± 0.189	1.581	>0.999
HS:F**C**A**V**V vs. HS:F**C**A**V**I	−0.144 ± 0.192	1.064	>0.999
HS:F**C**A**V**V vs. HS:FS**V**VI	1.448 ± 0.186	11.02	**<0.001**
HS:F**C**A**V**V vs. HS:FSA**V**V	−0.332 ± 0.189	2.490	0.929
HS:F**C**A**V**V vs. LS:FSA**V**I	0.573 ± 0.150	5.415	**0.013**
HS:F**C**A**V**V vs. LS:F**C**V**V**V	0.029 ± 0.174	0.239	>0.999
HS:F**C**A**V**V vs. LS:F**C**V**V**I	0.008 ± 0.176	0.063	>0.999
HS:F**C**A**V**V vs. LS:F**C**A**V**V	0.030 ± 0.187	0.229	>0.999
HS:F**C**A**V**V vs. LS:FS**V**V**V**	−0.110 ± 0.176	0.883	>0.999
HS:F**C**A**V**V vs. LS:F**C**A**V**I	−0.162 ± 0.187	1.223	>0.999
HS:F**C**A**V**V vs. LS:FS**V**VI	0.088 ± 0.174	0.717	>0.999
HS:F**C**A**V**V vs. LS:FSA**V**V	−0.038 ± 0.187	0.286	>0.999
HS:FS**V**V**V** vs. HS:F**C**A**V**I	−0.355 ± 0.193	2.599	0.902
HS:FS**V**V**V** vs. HS:FS**V**VI	1.237 ± 0.187	9.344	**<0.001**
HS:FS**V**V**V** vs. HS:FSA**V**V	−0.543 ± 0.190	4.040	0.240
HS:FS**V**V**V** vs. LS:FSA**V**I	0.362 ± 0.152	3.382	0.555
HS:FS**V**V**V** vs. LS:F**C**V**V**V	−0.182 ± 0.175	1.467	>0.999
HS:FS**V**V**V** vs. LS:F**C**V**V**I	−0.203 ± 0.178	1.618	0.999
HS:FS**V**V**V** vs. LS:F**C**A**V**V	−0.181 ± 0.189	1.354	>0.999
HS:FS**V**V**V** vs. LS:FS**V**V**V**	−0.321 ± 0.178	2.556	0.914
HS:FS**V**V**V** vs. LS:F**C**A**V**I	−0.373 ± 0.189	2.795	0.838
HS:FS**V**V**V** vs. LS:FS**V**VI	−0.123 ± 0.175	0.994	>0.999
HS:FS**V**V**V** vs. LS:FSA**V**V	−0.249 ± 0.189	1.865	0.995
HS:F**C**A**V**I vs. HS:FS**V**VI	1.593 ± 0.191	11.82	**<0.001**
HS:F**C**A**V**I vs. HS:FSA**V**V	−0.188 ± 0.193	1.374	0.999
HS:F**C**A**V**I vs. LS:FSA**V**I	0.718 ± 0.156	6.527	**<0.001**
HS:F**C**A**V**I vs. LS:F**C**V**V**V	0.174 ± 0.178	1.376	0.999
HS:F**C**A**V**I vs. LS:F**C**V**V**I	0.152 ± 0.181	1.189	>0.999
HS:F**C**A**V**I vs. LS:F**C**A**V**V	0.175 ± 0.192	1.287	>0.999
HS:F**C**A**V**I vs. LS:FS**V**V**V**	0.034 ± 0.181	0.269	>0.999
HS:F**C**A**V**I vs. LS:F**C**A**V**I	−0.018 ± 0.192	0.130	>0.999
HS:F**C**A**V**I vs. LS:FS**V**VI	0.232 ± 0.178	1.840	0.996
HS:F**C**A**V**I vs. LS:FSA**V**V	0.106 ± 0.192	0.784	>0.999
HS:FS**V**VI vs. HS:FSA**V**V	−1.780 ± 0.187	13.44	**<0.001**
HS:FS**V**VI vs. LS:FSA**V**I	−0.875 ± 0.148	8.361	**<0.001**
HS:FS**V**VI vs. LS:F**C**V**V**V	−1.419 ± 0.172	11.67	**<0.001**

Table S11B cont.			
Receptor Comparison	**Mean Difference ± SE**	**q**	**Adjusted *P* Value**
HS:FS**V**I vs. LS:F**C**V**V**I	−1.441 ± 0.175	11.67	**<0.001**
HS:FS**V**I vs. LS:F**C**A**V**	−1.418 ± 0.186	10.79	**<0.001**
HS:FS**V**I vs. LS:FS**V**V	−1.558 ± 0.175	12.63	**<0.001**
HS:FS**V**I vs. LS:F**C**AI	−1.610 ± 0.186	12.25	**<0.001**
HS:FS**V**I vs. LS:FS**V**I	−1.360 ± 0.172	11.19	**<0.001**
HS:FS**V**I vs. LS:FSA**V**	−1.486 ± 0.186	11.31	**<0.001**
HS:FSA**V** vs. LS:FSAI	0.905 ± 0.152	8.449	**<0.001**
HS:FSA**V** vs. LS:F**C**V**V**	0.361 ± 0.175	2.920	0.787
HS:FSA**V** vs. LS:F**C**V**I**	0.340 ± 0.178	2.708	0.869
HS:FSA**V** vs. LS:F**C**A**V**	0.362 ± 0.189	2.717	0.866
HS:FSA**V** vs. LS:FS**V**V	0.222 ± 0.178	1.770	0.997
HS:FSA**V** vs. LS:F**C**AI	0.170 ± 0.189	1.276	>0.999
HS:FSA**V** vs. LS:FS**V**I	0.420 ± 0.175	3.393	0.549
HS:FSA**V** vs. LS:FSA**V**	0.294 ± 0.189	2.205	0.977
LS:FSAI vs. LS:F**C**V**V**	−0.544 ± 0.132	5.821	**0.004**
LS:FSAI vs. LS:F**C**V**I**	−0.566 ± 0.136	5.904	**0.004**
LS:FSAI vs. LS:F**C**A**V**	−0.543 ± 0.150	5.128	**0.027**
LS:FSAI vs. LS:FS**V**V	−0.683 ± 0.136	7.133	**<0.001**
LS:FSAI vs. LS:F**C**AI	−0.735 ± 0.150	6.944	**<0.001**
LS:FSAI vs. LS:FS**V**I	−0.485 ± 0.132	5.194	**0.023**
LS:FSAI vs. LS:FSA**V**	−0.611 ± 0.150	5.773	**0.005**
LS:F**C**V**V** vs. LS:F**C**V**I**	−0.022 ± 0.161	0.189	>0.999
LS:F**C**V**V** vs. LS:F**C**A**V**	0.001 ± 0.174	0.008	>0.999
LS:F**C**V**V** vs. LS:FS**V**V	−0.139 ± 0.161	1.220	>0.999
LS:F**C**V**V** vs. LS:F**C**AI	−0.191 ± 0.172	1.559	>0.999
LS:F**C**V**V** vs. LS:FS**V**I	0.059 ± 0.159	0.523	>0.999
LS:F**C**V**V** vs. LS:FSA**V**	−0.067 ± 0.174	0.548	>0.999
LS:F**C**V**I** vs. LS:F**C**A**V**	0.023 ± 0.176	0.181	>0.999
LS:F**C**V**I** vs. LS:FS**V**V	−0.118 ± 0.164	1.015	>0.999
LS:F**C**V**I** vs. LS:F**C**AI	−0.170 ± 0.176	1.364	>0.999
LS:F**C**V**I** vs. LS:FS**V**I	0.080 ± 0.161	0.702	>0.999
LS:F**C**V**I** vs. LS:FSA**V**	−0.046 ± 0.176	0.367	>0.999
LS:F**C**A**V** vs. LS:FS**V**V	−0.140 ± 0.176	1.127	>0.999
LS:F**C**A**V** vs. LS:F**C**AI	−0.192 ± 0.187	1.452	0.997
LS:F**C**A**V** vs. LS:FS**V**I	0.058 ± 0.174	0.470	>0.999
LS:F**C**A**V** vs. LS:FSA**V**	−0.068 ± 0.187	0.515	>0.999
LS:FS**V**V vs. LS:F**C**AI	−0.052 ± 0.176	0.418	>0.999
LS:FS**V**V vs. LS:FS**V**I	0.198 ± 0.161	1.734	0.998
LS:FS**V**V vs. LS:FSA**V**	0.072 ± 0.176	0.579	>0.999
LS:F**C**AI vs. LS:FS**V**I	0.250 ± 0.174	2.037	0.988
LS:F**C**AI vs. LS:FSA**V**	0.124 ± 0.187	0.937	>0.999
LS:FS**V**I vs. LS:FSA**V**	−0.129 ± 0.174	1.026	>0.999

Table S12. Statistical comparisons of the effect of receptor stoichiometry and genotype on response to epibatidine (maximal current) of Human-to-*Ameerega* mutated nAChRs. HS: high sensitivity (1:7 ratio); LS: low sensitivity (7:1 ratio).

A. Two-way ANOVA

Source of Variation	% of total variation	SS (Type III)	DF	MS	F (DFn, DFd)	*P* value
Interaction	14.11	5539626	7	791375	F (7, 719) = 25.58	<0.001
Stoichiometry (HS vs. LS)	13.37	5248866	1	5248866	F (1, 719) = 169.7	<0.001
Receptor Genotype	15.83	6214085	7	887726	F (7, 719) = 28.69	<0.001
Residual		22244317	719	30938		

B. Tukey's multiple comparisons test.

Receptor Comparison	Mean Difference ± SE	q	Adjusted *P* Value
HS:FSAI vs. HS:F**C**V**V**	9.710 ± 32.95	0.417	>0.999
HS:FSAI vs. HS:F**C**V**I**	−53.04 ± 32.95	2.276	0.967
HS:FSAI vs. HS:F**C**A**V**	−32.84 ± 35.36	1.314	>0.999
HS:FSAI vs. HS:FS**V**V	−207.6 ± 35.77	8.210	**<0.001**
HS:FSAI vs. HS:F**C**AI	−65.34 ± 36.66	2.521	0.922
HS:FSAI vs. HS:FS**V**I	0.720 ± 34.96	0.029	>0.999
HS:FSAI vs. HS:FSA**V**	−112.7 ± 35.77	4.458	0.116
HS:FSAI vs. LS:FSAI	−345.7 ± 23.97	20.40	**<0.001**
HS:FSAI vs. LS:F**C**V**V**	−78.24 ± 31.39	3.525	0.478
HS:FSAI vs. LS:F**C**V**I**	−106.8 ± 32.12	4.703	0.071
HS:FSAI vs. LS:F**C**A**V**	−82.94 ± 35.36	3.318	0.589
HS:FSAI vs. LS:FS**V**V	−386.9 ± 32.12	17.03	**<0.001**
HS:FSAI vs. LS:F**C**AI	−79.44 ± 35.36	3.178	0.663
HS:FSAI vs. LS:FS**V**I	−604.5 ± 31.39	27.24	**<0.001**
HS:FSAI vs. LS:FSA**V**	−234.5 ± 35.36	9.382	**<0.001**
HS:F**C**V**V** vs. HS:F**C**V**I**	−62.75 ± 39.33	2.256	0.969
HS:F**C**V**V** vs. HS:F**C**A**V**	−42.55 ± 41.36	1.455	>0.999
HS:F**C**V**V** vs. HS:FS**V**V	−217.4 ± 41.72	7.368	**<0.001**
HS:F**C**V**V** vs. HS:F**C**AI	−75.05 ± 42.48	2.498	0.927
HS:F**C**V**V** vs. HS:FS**V**I	−8.990 ± 41.03	0.310	>0.999
HS:F**C**V**V** vs. HS:FSA**V**	−122.5 ± 41.72	4.151	0.200
HS:F**C**V**V** vs. LS:FSAI	−355.5 ± 32.18	15.62	**<0.001**
HS:F**C**V**V** vs. LS:F**C**V**V**	−87.95 ± 38.03	3.271	0.614
HS:F**C**V**V** vs. LS:F**C**V**I**	−116.6 ± 38.64	4.266	0.165
HS:F**C**V**V** vs. LS:F**C**A**V**	−92.65 ± 41.36	3.168	0.668
HS:F**C**V**V** vs. LS:FS**V**V	−396.7 ± 38.64	14.52	**<0.001**
HS:F**C**V**V** vs. LS:F**C**AI	−89.15 ± 41.36	3.048	0.728
HS:F**C**V**V** vs. LS:FS**V**I	−614.3 ± 38.03	22.84	**<0.001**
HS:F**C**V**V** vs. LS:FSA**V**	−244.3 ± 41.36	8.351	**<0.001**
HS:F**C**V**I** vs. HS:F**C**A**V**	20.20 ± 41.36	0.691	>0.999

Table S12B cont.			
Receptor Comparison	**Mean Difference ± SE**	**q**	**Adjusted *P* Value**
HS:F**C**V**V**I vs. HS:FS**V**V	−154.6 ± 41.72	5.241	**0.021**
HS:F**C**V**V**I vs. HS:F**C**AI	−12.30 ± 42.48	0.410	>0.999
HS:F**C**V**V**I vs. HS:FS**V**I	53.76 ± 41.03	1.853	0.996
HS:F**C**V**V**I vs. HS:FSA**V**	−59.70 ± 41.72	2.024	0.989
HS:F**C**V**V**I vs. LS:FSAI	−292.7 ± 32.18	12.86	**<0.001**
HS:F**C**V**V**I vs. LS:F**C**V**V**	−25.20 ± 38.03	0.937	>0.999
HS:F**C**V**V**I vs. LS:F**C**V**V**I	−53.80 ± 38.64	1.969	0.992
HS:F**C**V**V**I vs. LS:F**C**A**V**	−29.90 ± 41.36	1.022	>0.999
HS:F**C**V**V**I vs. LS:FS**V**V	−333.9 ± 38.64	12.22	**<0.001**
HS:F**C**V**V**I vs. LS:F**C**AI	−26.40 ± 41.36	0.903	>0.999
HS:F**C**V**V**I vs. LS:FS**V**I	−551.5 ± 38.03	20.51	**<0.001**
HS:F**C**V**V**I vs. LS:FSA**V**	−181.5 ± 41.36	6.205	**0.001**
HS:F**C**A**V** vs. HS:FS**V**V	−174.8 ± 43.64	5.665	**0.007**
HS:F**C**A**V** vs. HS:F**C**AI	−32.50 ± 44.37	1.036	>0.999
HS:F**C**A**V** vs. HS:FS**V**I	33.56 ± 42.98	1.104	>0.999
HS:F**C**A**V** vs. HS:FSA**V**	−79.90 ± 43.64	2.589	0.905
HS:F**C**A**V** vs. LS:FSAI	−312.9 ± 34.64	12.78	**<0.001**
HS:F**C**A**V** vs. LS:F**C**V**V**	−45.40 ± 40.13	1.600	0.999
HS:F**C**A**V** vs. LS:F**C**V**I**	−74.00 ± 40.71	2.571	0.910
HS:F**C**A**V** vs. LS:F**C**A**V**	−50.10 ± 43.30	1.636	0.999
HS:F**C**A**V** vs. LS:FS**V**V	−354.1 ± 40.71	12.30	**<0.001**
HS:F**C**A**V** vs. LS:F**C**AI	−46.60 ± 43.30	1.522	>0.999
HS:F**C**A**V** vs. LS:FS**V**I	−571.7 ± 40.13	20.15	**<0.001**
HS:F**C**A**V** vs. LS:FSA**V**	−201.7 ± 43.30	6.587	**<0.001**
HS:FS**V**V vs. HS:F**C**AI	142.3 ± 44.70	4.502	0.106
HS:FS**V**V vs. HS:FS**V**I	208.4 ± 43.32	6.802	**<0.001**
HS:FS**V**V vs. HS:FSA**V**	94.90 ± 43.97	3.052	0.726
HS:FS**V**V vs. LS:FSAI	−138.1 ± 35.06	5.571	**0.009**
HS:FS**V**V vs. LS:F**C**V**V**	129.4 ± 40.49	4.520	0.103
HS:FS**V**V vs. LS:F**C**V**I**	100.8 ± 41.06	3.471	0.507
HS:FS**V**V vs. LS:F**C**A**V**	124.7 ± 43.64	4.041	0.239
HS:FS**V**V vs. LS:FS**V**V	−179.3 ± 41.06	6.175	**0.002**
HS:FS**V**V vs. LS:F**C**AI	128.2 ± 43.64	4.155	0.199
HS:FS**V**V vs. LS:FS**V**I	−396.9 ± 40.49	13.86	**<0.001**
HS:FS**V**V vs. LS:FSA**V**	−26.90 ± 43.64	0.872	>0.999
HS:F**C**AI vs. HS:FS**V**I	66.06 ± 44.06	2.120	0.983
HS:F**C**AI vs. HS:FSA**V**	−47.40 ± 44.70	1.500	>0.999
HS:F**C**AI vs. LS:FSAI	−280.4 ± 35.96	11.03	**<0.001**
HS:F**C**AI vs. LS:F**C**V**V**	−12.90 ± 41.28	0.442	>0.999
HS:F**C**AI vs. LS:F**C**V**I**	−41.50 ± 41.84	1.403	>0.999
HS:F**C**AI vs. LS:F**C**A**V**	−17.60 ± 44.37	0.561	>0.999
HS:F**C**AI vs. LS:FS**V**V	−321.6 ± 41.84	10.87	**<0.001**
HS:F**C**AI vs. LS:F**C**AI	−14.10 ± 44.37	0.449	>0.999
HS:F**C**AI vs. LS:FS**V**I	−539.2 ± 41.28	18.47	**<0.001**
HS:F**C**AI vs. LS:FSA**V**	−169.2 ± 44.37	5.393	**0.014**

Table S12B cont.			
Receptor Comparison	**Mean Difference ± SE**	**q**	**Adjusted *P* Value**
HS:FS**V**I vs. HS:FSA**V**	−113.5 ± 43.32	3.704	0.387
HS:FS**V**I vs. LS:FSAI	−346.5 ± 34.24	14.31	**<0.001**
HS:FS**V**I vs. LS:F**C**V**V**	−78.96 ± 39.78	2.807	0.833
HS:FS**V**I vs. LS:F**C**V**I**	−107.6 ± 40.37	3.768	0.356
HS:FS**V**I vs. LS:F**C**A**V**	−83.66 ± 42.98	2.753	0.853
HS:FS**V**I vs. LS:FS**V**V	−387.7 ± 40.37	13.58	**<0.001**
HS:FS**V**I vs. LS:F**C**AI	−80.16 ± 42.98	2.637	0.891
HS:FS**V**I vs. LS:FS**V**I	−605.3 ± 39.78	21.52	**<0.001**
HS:FS**V**I vs. LS:FSA**V**	−235.3 ± 42.98	7.741	**<0.001**
HS:FSA**V** vs. LS:FSAI	−233.0 ± 35.06	9.399	**<0.001**
HS:FSA**V** vs. LS:F**C**V**V**	34.50 ± 40.49	1.205	>0.999
HS:FSA**V** vs. LS:F**C**V**I**	5.900 ± 41.06	0.203	>0.999
HS:FSA**V** vs. LS:F**C**A**V**	29.80 ± 43.64	0.967	>0.999
HS:FSA**V** vs. LS:FS**V**V	−274.2 ± 41.06	9.443	**<0.001**
HS:FSA**V** vs. LS:F**C**AI	33.30 ± 43.64	1.079	>0.999
HS:FSA**V** vs. LS:FS**V**I	−491.8 ± 40.49	17.18	**<0.001**
HS:FSA**V** vs. LS:FSA**V**	−121.8 ± 43.64	3.947	0.277
LS:FSAI vs. LS:F**C**V**V**	267.5 ± 30.57	12.37	**<0.001**
LS:FSAI vs. LS:F**C**V**I**	238.9 ± 31.33	10.78	**<0.001**
LS:FSAI vs. LS:F**C**A**V**	262.8 ± 34.64	10.73	**<0.001**
LS:FSAI vs. LS:FS**V**V	−41.20 ± 31.33	1.860	0.995
LS:FSAI vs. LS:F**C**AI	266.3 ± 34.64	10.87	**<0.001**
LS:FSAI vs. LS:FS**V**I	−258.8 ± 30.57	11.97	**<0.001**
LS:FSAI vs. LS:FSA**V**	111.2 ± 34.64	4.540	0.098
LS:F**C**V**V** vs. LS:F**C**V**I**	−28.60 ± 37.31	1.084	>0.999
LS:F**C**V**V** vs. LS:F**C**A**V**	−4.700 ± 40.13	0.166	>0.999
LS:F**C**V**V** vs. LS:FS**V**V	−308.7 ± 37.31	11.70	**<0.001**
LS:F**C**V**V** vs. LS:F**C**AI	−1.200 ± 40.13	0.043	>0.999
LS:F**C**V**V** vs. LS:FS**V**I	−526.3 ± 36.68	20.29	**<0.001**
LS:F**C**V**V** vs. LS:FSA**V**	−156.3 ± 40.13	5.509	**0.010**
LS:F**C**V**I** vs. LS:F**C**A**V**	23.90 ± 40.71	0.830	>0.999
LS:F**C**V**I** vs. LS:FS**V**V	−280.1 ± 37.93	10.44	**<0.001**
LS:F**C**V**I** vs. LS:F**C**AI	27.40 ± 40.71	0.952	>0.999
LS:F**C**V**I** vs. LS:FS**V**I	−497.7 ± 37.31	18.86	**<0.001**
LS:F**C**V**I** vs. LS:FSA**V**	−127.7 ± 40.71	4.437	0.120
LS:F**C**A**V** vs. LS:FS**V**V	−304.0 ± 40.71	10.56	**<0.001**
LS:F**C**A**V** vs. LS:F**C**AI	3.500 ± 43.30	0.114	>0.999
LS:F**C**A**V** vs. LS:FS**V**I	−521.6 ± 40.13	18.38	**<0.001**
LS:F**C**A**V** vs. LS:FSA**V**	−151.6 ± 43.30	4.951	**0.041**
LS:FS**V**V vs. LS:F**C**AI	307.5 ± 40.71	10.68	**<0.001**
LS:FS**V**V vs. LS:FS**V**I	−217.6 ± 37.31	8.248	**<0.001**
LS:FS**V**V vs. LS:FSA**V**	152.4 ± 40.71	5.295	**0.018**
LS:F**C**AI vs. LS:FS**V**I	−525.1 ± 40.13	18.51	**<0.001**
LS:F**C**AI vs. LS:FSA**V**	−155.1 ± 43.30	5.066	**0.031**
LS:FS**V**I vs. LS:FSA**V**	370.0 ± 40.13	13.04	**<0.001**

Table S13. Statistical comparisons of the effect of receptor stoichiometry and genotype on response to ACh (logEC_{50}) of *Epipedobates*-to-Human mutated nAChRs. HS: high sensitivity (1:7 ratio); LS: low sensitivity (7:1 ratio).

A. Two-way ANOVA

Source of Variation	% of total variation	SS (Type III)	DF	MS	F (DFn, DFd)	*P* value
Interaction	0.641	0.336	3	0.112	F (3, 385) = 0.906	0.438
Stoichiometry (HS vs. LS)	0.087	0.046	1	0.046	F (1, 385) = 0.368	0.544
Receptor Genotype	8.464	4.437	3	1.479	F (3, 385) = 11.96	<0.001
Residual		47.60	385	0.124		

B. Tukey's multiple comparisons test.

Receptor Comparison	Mean Difference ± SE	q	Adjusted *P* Value
HS:**FS**AI vs. HS:LCAI	0.012 ± 0.069	0.244	>0.999
HS:**FS**AI vs. HS:**F**CAI	−0.302 ± 0.080	5.338	**0.005**
HS:**FS**AI vs. HS:L**S**AI	−0.068 ± 0.081	1.173	0.991
HS:**FS**AI vs. LS:**FS**AI	−0.122 ± 0.078	2.205	0.774
HS:**FS**AI vs. LS:LCAI	−0.014 ± 0.065	0.305	>0.999
HS:**FS**AI vs. LS:**F**CAI	−0.280 ± 0.075	5.246	**0.006**
HS:**FS**AI vs. LS:L**S**AI	−0.032 ± 0.079	0.570	>0.999
HS:LCAI vs. HS:**F**CAI	−0.314 ± 0.073	6.085	**<0.001**
HS:LCAI vs. HS:L**S**AI	−0.079 ± 0.074	1.511	0.963
HS:LCAI vs. LS:**FS**AI	−0.134 ± 0.071	2.666	0.562
HS:LCAI vs. LS:LCAI	−0.026 ± 0.057	0.652	>0.999
HS:LCAI vs. LS:**F**CAI	−0.292 ± 0.068	6.072	**<0.001**
HS:LCAI vs. LS:L**S**AI	−0.044 ± 0.072	0.863	0.999
HS:**F**CAI vs. HS:L**S**AI	0.234 ± 0.084	3.938	0.102
HS:**F**CAI vs. LS:**FS**AI	0.180 ± 0.081	3.125	0.348
HS:**F**CAI vs. LS:LCAI	0.287 ± 0.069	5.888	**0.001**
HS:**F**CAI vs. LS:**F**CAI	0.022 ± 0.079	0.389	>0.999
HS:**F**CAI vs. LS:L**S**AI	0.270 ± 0.082	4.665	**0.023**
HS:L**S**AI vs. LS:**FS**AI	−0.055 ± 0.083	0.934	0.998
HS:L**S**AI vs. LS:LCAI	0.053 ± 0.071	1.068	0.995
HS:L**S**AI vs. LS:**F**CAI	−0.213 ± 0.080	3.762	0.138
HS:L**S**AI vs. LS:L**S**AI	0.036 ± 0.083	0.607	>0.999
LS:**FS**AI vs. LS:LCAI	0.108 ± 0.067	2.273	0.746
LS:**FS**AI vs. LS:**F**CAI	−0.158 ± 0.077	2.904	0.448
LS:**FS**AI vs. LS:L**S**AI	0.090 ± 0.080	1.592	0.951
LS:LCAI vs. LS:**F**CAI	−0.266 ± 0.064	5.886	**0.001**
LS:LCAI vs. LS:L**S**AI	−0.018 ± 0.068	0.368	>0.999
LS:**F**CAI vs. LS:L**S**AI	0.248 ± 0.077	4.530	**0.032**

Table S14. Statistical comparisons of the effect of receptor stoichiometry and genotype on response to epibatidine (logEC_{50}) of *Epipedobates*-to-Human mutated nAChRs. HS: high sensitivity (1:7 ratio); LS: low sensitivity (7:1 ratio).

A. Two-way ANOVA

Source of Variation	% of total variation	SS (Type III)	DF	MS	F (DFn, DFd)	*P* value
Interaction	0.024	0.262	3	0.087	F (3, 270) = 0.098	0.961
Stoichiometry (HS vs. LS)	59.61	651.2	1	651.2	F (1, 270) = 726.6	<0.001
Receptor Genotype	18.22	199.0	3	66.35	F (3, 270) = 74.03	<0.001
Residual		242.0	270	0.896		

B. Tukey's multiple comparisons test.

Receptor Comparison	Mean Difference ± SE	q	Adjusted *P* Value
HS:**FS**AI vs. HS:LCAI	−1.638 ± 0.241	9.597	**<0.001**
HS:**FS**AI vs. HS:**F**CAI	−2.134 ± 0.258	11.68	**<0.001**
HS:**FS**AI vs. HS:L**S**AI	−0.246 ± 0.277	1.257	0.987
HS:**FS**AI vs. LS:**FS**AI	−3.311 ± 0.237	19.75	**<0.001**
HS:**FS**AI vs. LS:LCAI	−4.864 ± 0.232	29.66	**<0.001**
HS:**FS**AI vs. LS:**F**CAI	−5.287 ± 0.274	27.34	**<0.001**
HS:**FS**AI vs. LS:L**S**AI	−3.401 ± 0.236	20.37	**<0.001**
HS:LCAI vs. HS:**F**CAI	−0.496 ± 0.231	3.038	0.387
HS:LCAI vs. HS:L**S**AI	1.392 ± 0.251	7.834	**<0.001**
HS:LCAI vs. LS:**FS**AI	−1.673 ± 0.207	11.44	**<0.001**
HS:LCAI vs. LS:LCAI	−3.226 ± 0.201	22.72	**<0.001**
HS:LCAI vs. LS:**F**CAI	−3.649 ± 0.248	20.83	**<0.001**
HS:LCAI vs. LS:L**S**AI	−1.763 ± 0.206	12.12	**<0.001**
HS:**F**CAI vs. HS:L**S**AI	1.888 ± 0.268	9.975	**<0.001**
HS:**F**CAI vs. LS:**FS**AI	−1.177 ± 0.226	7.348	**<0.001**
HS:**F**CAI vs. LS:LCAI	−2.730 ± 0.221	17.47	**<0.001**
HS:**F**CAI vs. LS:**F**CAI	−3.153 ± 0.264	16.87	**<0.001**
HS:**F**CAI vs. LS:L**S**AI	−1.267 ± 0.225	7.950	**<0.001**
HS:L**S**AI vs. LS:**FS**AI	−3.065 ± 0.247	17.53	**<0.001**
HS:L**S**AI vs. LS:LCAI	−4.618 ± 0.242	26.96	**<0.001**
HS:L**S**AI vs. LS:**F**CAI	−5.041 ± 0.282	25.25	**<0.001**
HS:L**S**AI vs. LS:L**S**AI	−3.155 ± 0.246	18.12	**<0.001**
LS:**FS**AI vs. LS:LCAI	−1.554 ± 0.196	11.23	**<0.001**
LS:**FS**AI vs. LS:**F**CAI	−1.977 ± 0.244	11.47	**<0.001**
LS:**FS**AI vs. LS:L**S**AI	−0.091 ± 0.201	0.639	>0.999
LS:LCAI vs. LS:**F**CAI	−0.423 ± 0.239	2.508	0.637
LS:LCAI vs. LS:L**S**AI	1.463 ± 0.195	10.63	**<0.001**
LS:**F**CAI vs. LS:L**S**AI	1.886 ± 0.243	10.99	**<0.001**

Table S15. Statistical comparisons of the effect of receptor stoichiometry and genotype on response to epibatidine (maximal current expressed as percentage of ACh maximal current) of *Epipedobates*-to-Human mutated nAChRs. HS: high sensitivity (1:7 ratio); LS: low sensitivity (7:1 ratio).

A. Two-way ANOVA

Source of Variation	% of total variation	SS (Type III)	DF	MS	F (DFn, DFd)	*P* value
Interaction	6.313	73640	3	24547	F (3, 270) = 6.849	<0.001
Stoichiometry (HS vs. LS)	5.350	62402	1	62402	F (1, 270) = 17.41	<0.001
Receptor Genotype	5.382	62780	3	20927	F (3, 270) = 5.839	<0.001
Residual		967634	270	3584		

B. Tukey's multiple comparisons test.

Receptor Comparison	Mean Difference ± SE	*q*	Adjusted *P* Value
HS:**FS**AI vs. HS:LCAI	39.65 ± 15.26	3.674	0.161
HS:**FS**AI vs. HS:**F**CAI	40.25 ± 16.34	3.484	0.216
HS:**FS**AI vs. HS:L**S**AI	15.14 ± 17.50	1.223	0.989
HS:**FS**AI vs. LS:**FS**AI	20.16 ± 14.99	1.902	0.881
HS:**FS**AI vs. LS:LCAI	−24.60 ± 14.66	2.372	0.702
HS:**FS**AI vs. LS:**F**CAI	18.78 ± 17.30	1.536	0.959
HS:**FS**AI vs. LS:L**S**AI	−45.04 ± 14.93	4.265	0.056
HS:LCAI vs. HS:**F**CAI	0.600 ± 14.60	0.058	>0.999
HS:LCAI vs. HS:L**S**AI	−24.51 ± 15.89	2.181	0.784
HS:LCAI vs. LS:**FS**AI	−19.49 ± 13.08	2.108	0.812
HS:LCAI vs. LS:LCAI	−64.25 ± 12.70	7.155	**<0.001**
HS:LCAI vs. LS:**F**CAI	−20.87 ± 15.67	1.884	0.886
HS:LCAI vs. LS:L**S**AI	−84.69 ± 13.01	9.207	**<0.001**
HS:**F**CAI vs. HS:L**S**AI	−25.11 ± 16.93	2.098	0.816
HS:**F**CAI vs. LS:**FS**AI	−20.09 ± 14.32	1.984	0.855
HS:**F**CAI vs. LS:LCAI	−64.85 ± 13.97	6.563	**0.001**
HS:**F**CAI vs. LS:**F**CAI	−21.47 ± 16.72	1.816	0.904
HS:**F**CAI vs. LS:L**S**AI	−85.29 ± 14.26	8.461	**<0.001**
HS:L**S**AI vs. LS:**FS**AI	5.020 ± 15.63	0.454	>0.999
HS:L**S**AI vs. LS:LCAI	−39.74 ± 15.32	3.669	0.162
HS:L**S**AI vs. LS:**F**CAI	3.640 ± 17.85	0.288	>0.999
HS:L**S**AI vs. LS:L**S**AI	−60.18 ± 15.57	5.465	**0.004**
LS:**FS**AI vs. LS:LCAI	−44.76 ± 12.37	5.115	**0.008**
LS:**FS**AI vs. LS:**F**CAI	−1.380 ± 15.40	0.127	>0.999
LS:**FS**AI vs. LS:L**S**AI	−65.20 ± 12.69	7.265	**<0.001**
LS:LCAI vs. LS:**F**CAI	43.38 ± 15.08	4.067	0.082
LS:LCAI vs. LS:L**S**AI	−20.44 ± 12.30	2.350	0.712
LS:**F**CAI vs. LS:L**S**AI	−63.82 ± 15.34	5.882	**0.001**

Table S16. Statistical comparisons of the effect of receptor stoichiometry and genotype on response to ACh (log*EC*$_{50}$) from Human/*Epipedobates* combinations. Human (*H*) wild-type α4β2 nAChRs [α4(D) and β2(FSAI) genotypes], *Epipedobates* (*E*) wild-type α4β2 nAChRs [α4(N) and β2(LCAI) genotypes], and combinations incorporating the mirror AA replacement patterns in α4 (**D** and **N**), as well as the *Epipedobates* β2(**F**CAI) genotype. For biphasic curves, only the low sensitivity EC_{50} was included (see statistic section). α4:β2 cRNA ratio 7:1.

A. One-way ANOVA

ANOVA table	SS	DF	MS	F (DFn, DFd)	*P* value
Treatment (between columns)	480.4	6	80.06	F (6, 283) = 93.21	<0.001
Residual (within columns)	243.1	283	0.8589		
Total	723.4	289			

B. Tukey's multiple comparisons test

Receptor Comparison	Mean Difference ± SE	q	Adjusted *P* Value
E α4(N) *E* β2(LCAI) vs. *E* α4(**D**) *E* β2(LCAI)	0.022 ± 0.230	0.136	>0.999
E α4(N) *E* β2(LCAI) vs. *E* α4(N) *H* β2(FSAI)	0.171 ± 0.222	1.085	0.988
E α4(N) *E* β2(LCAI) vs. *H* α4(D) *H* β2(FSAI)	−2.602 ± 0.248	14.86	**<0.001**
E α4(N) *E* β2(LCAI) vs. *H* α4(**N**) *H* β2(FSAI)	−2.938 ± 0.212	19.64	**<0.001**
E α4(N) *E* β2(LCAI) vs. *H* α4(D) *E* β2(LCAI)	−1.763 ± 0.218	11.44	**<0.001**
E α4(N) *E* β2(LCAI) vs. *H* α4(D) *E* β2(**F**CAI)	−2.477 ± 0.232	15.09	**<0.001**
E α4(**D**) *E* β2(LCAI) vs. *E* α4(N) *H* β2(FSAI)	0.148 ± 0.202	1.040	0.990
E α4(**D**) *E* β2(LCAI) vs. *H* α4(D) *H* β2(FSAI)	−2.624 ± 0.230	16.17	**<0.001**
E α4(**D**) *E* β2(LCAI) vs. *H* α4(**N**) *H* β2(FSAI)	−2.960 ± 0.190	22.03	**<0.001**
E α4(**D**) *E* β2(LCAI) vs. *H* α4(D) *E* β2(LCAI)	−1.785 ± 0.197	12.81	**<0.001**
E α4(**D**) *E* β2(LCAI) vs. *H* α4(D) *E* β2(**F**CAI)	−2.499 ± 0.213	16.62	**<0.001**
E α4(N) *H* β2(FSAI) vs. *H* α4(D) *H* β2(FSAI)	−2.773 ± 0.222	17.65	**<0.001**
E α4(N) *H* β2(FSAI) vs. *H* α4(**N**) *H* β2(FSAI)	−3.109 ± 0.181	24.29	**<0.001**
E α4(N) *H* β2(FSAI) vs. *H* α4(D) *E* β2(LCAI)	−1.934 ± 0.188	14.51	**<0.001**
E α4(N) *H* β2(FSAI) vs. *H* α4(D) *E* β2(**F**CAI)	−2.648 ± 0.205	18.29	**<0.001**
H α4(D) *H* β2(FSAI) vs. *H* α4(**N**) *H* β2(FSAI)	−0.336 ± 0.212	2.246	0.690
H α4(D) *H* β2(FSAI) vs. *H* α4(D) *E* β2(LCAI)	0.839 ± 0.218	5.443	**0.003**
H α4(D) *H* β2(FSAI) vs. *H* α4(D) *E* β2(**F**CAI)	0.125 ± 0.232	0.762	0.998
H α4(**N**) *H* β2(FSAI) vs. *H* α4(D) *E* β2(LCAI)	1.175 ± 0.176	9.450	**<0.001**
H α4(**N**) *H* β2(FSAI) vs. *H* α4(D) *E* β2(**F**CAI)	0.461 ± 0.193	3.376	0.208
H α4(D) *E* β2(LCAI) vs. *H* α4(D) *E* β2(**F**CAI)	−0.714 ± 0.200	5.045	**0.008**

Additional Data table S1 (separate file)

Chrnb2_alignment.nex: Nexus alignment of chrnb2 nucleotide sequences
Chrna4_alignment.nex: Nexus alignment of chrna4 nucleotide sequences